Multipoint correlation functions for continuous-time random walk models of anomalous diffusion

František Šanda and Shaul Mukamel*
Department of Chemistry, University of California, Irvine, California 92697, USA
(Received 26 April 2005; published 27 September 2005)

Recursive relations are developed for computing the multipoint correlation functions of a particle undergoing a biased continuous-time random walk (CTRW) in an external potential. Two- and three-point correlation functions are calculated for waiting-time distributions with an anomalous power-law profile $t^{-\alpha-1}$, $0<\alpha<1$, on intermediate time scales with a crossover to an exponential long time decay. Comparison of the CTRW with the Brownian harmonic oscillator model (Gaussian process) illustrates how higher-order correlation functions may be used to distinguish between dynamical models that have the same two-point correlation function.

DOI: 10.1103/PhysRevE.72.031108 PACS number(s): 05.40.Fb, 02.50.−r

I. INTRODUCTION

Classical diffusion may be described by various models, including random walks, or Langevin, Fokker-Planck, or master equations [1,2]. Assuming short time correlations of the random force, the mean square displacement grows asymptotically linearly with time, $\langle[r(t)-r(0)]^2\rangle \propto t$ independent of the details of the model. The diffusion trajectories are self-similar with fractal characteristics—they are continuous and nondifferentiable [3,4].

Dynamical models of complex systems often lead to nonexponential relaxation with correlation functions decaying as stretched exponentials $C(t)\propto\exp(-t^{\beta})$ or power laws $C(t)\propto t^{-\alpha}$.When the time intervals between diffusive moves have fractal characteristics, the mean squared displacement of free diffusion can scale as $\langle[r(t)-r(0)]^2\rangle \propto t^{\gamma}$ [4,5]. This behavior is known as anomalous diffusion [6].

Non-subexponential relaxations were reported in many physical systems including charge-carrier transport, geophysical processes, biological systems, and economics [6–8]. Stochastic trajectories of single protein molecules and quantum dots show stretched-exponential or power-law kinetics and relaxation [9–20]. Long algebraic tails common to many complex systems (e.g., glasses, proteins, and supercooled liquids) are signatures of a complex energy landscape [21–23] with multiple barriers where the system has a broad distribution of time scales and may not be equilibrated on the relevant experimental time scales. Time-averaged correlation functions were applied [24,25] to anomalous on-off fluorescence statistics observed in single quantum dots [14,15].

Most studies so far focused on two-point correlation functions. This paper studies multipoint correlations which provide critical tests for the microscopic models underlying the anomalous relaxation [26–28]. Two-time properties of anomalous diffusion have been calculated using fractional Brownian motion [27–29], the diffusion equation [30], the Langevin equation [31,32], master equations (GME) [33,34], the age-dependent master equation (ADME) [35,36], and the continuous-time random walk (CTRW) [2,37]. Gaussian processes (GPs) are completely determined by their two-point correlation functions $C(\tau_1,\tau_0)\equiv\langle x(\tau_1)x(\tau_0)\rangle$; higher-order correlation functions carry no additional information and both regular and anomalous relaxation can be treated with the same formalism [38]. For example, the four-point correlation function of a Gaussian coordinate x is given by a sum of possible pairings:

$$\begin{aligned}\langle x(\tau_4)x(\tau_3)x(\tau_2)x(\tau_1)\rangle &= \langle x(\tau_4)x(\tau_3)\rangle\langle x(\tau_2)x(\tau_1)\rangle \\ &+ \langle x(\tau_4)x(\tau_2)\rangle\langle x(\tau_3)x(\tau_1)\rangle \\ &+ \langle x(\tau_4)x(\tau_1)\rangle\langle x(\tau_3)x(\tau_2)\rangle.\end{aligned}$$

The CTRW generalizes the ordinary random walk by introducing a waiting-time distribution (WTD) $\psi(t)$ between successive jumps. Broad distributions of step lengths (Lévy flights) [6,39] have been studied as well but will not be considered here. The CTRW model for transport was introduced by Montroll and Weiss [40,41]. It is equivalent to a master equation [33,42] as well as to a multistate trapping problem, when internal states of the particlar are associated with different hopping rates [43–45]. The dynamics of the internal space is assumed to be Markovian, so that the CTRW can be viewed as a projection of a Markovian process into a lower-dimensional space. The stochastic Liouville equations (SLEs), developed by Kubo [46–48], provide a useful tool for computing the multitime properties of the CTRW by a judicious choice of additional dynamical variables which map them into a Markovian process [49–51]. Similarly, the ADME approach introduces an additional variable which describes the time from the last jump ("age") and uses age-dependent rates to construct a Markovian description of the CTRW [35,36].

The CTRW in a harmonic potential and the anomalous GP are nonequivalent dynamical models. In both cases the subexponential decay is caused by the presence of different time scales for relaxation in the system. However, in the CTRW these time scales are realized sequentially. In contrast, an overdamped Gaussian variable can be decomposed as $x(t)=\Sigma_j x_j(t)$ where x_j are independent Uhlenbeck-Ornstein variables $\langle x_j(\tau_1)x_j(\tau_0)\rangle \sim e^{(\tau_1-\tau_0)/T_j}$ with different relaxation times T_j [38].

Two types of CTRW ensembles are commonly considered. By assuming that all particles made a jump at the time

*Email address: smukamel@uci.edu

origin we obtain a nonstationary process (NP). A WTD with infinite mean corresponding to anomalous diffusion was first applied to electron transport in amorphous semiconductors [52,53]. Starting with an ensemble of just arriving particles, gradually most of them are captured by deep traps with long waiting times and the system is never equilibrated. This effect is known as aging.

A stationary process (SP) must have a special WTD for the first jump, and can only be established for WTDs with a finite mean $\bar{t}=\int_0^\infty t\psi(t)dt$ [54]. For WTDs with finite first and second moments we expect a narrow Gaussian distribution of waiting times for a large number of steps (the central limit theorem) [6]. A macroscopic move requires an infinite number of short steps and the CTRW may be described by an ordinary diffusion equation at long times, independent of the details of the WTD. The above considerations do not apply when the waiting-time distribution for a few steps is broad, and anomalous relaxation occurs at intermediate time scales. The fundamental differences between the two ensembles have been known since the 1970s, when the frequency sensitivity (insensitivity) of ac conductivity was reported for NPs (SPs) [55,56].

Long-tailed WTDs with $\psi(t)\sim 1/t^{1+\alpha}$, $\alpha>0$, have been studied recently [57,58]. For $\alpha>1$ the first moment is finite. The first moment diverges for $0<\alpha<1$ and step function [57] or exponential long-time decay cutoffs [58] have been added to keep it finite. A two-state SP was recently applied to model the absorption line shape [58] and fluorescence on-off blinking statistics [57].

In this paper we analyze multipoint correlation functions of biased CTRWs in a potential with an anomalous WTD [7,59]. Two-point quantities for NPs in a harmonic potential with infinite $\bar{t}$ have been calculated using the fractional Fokker-Planck equation (FFPE) [60] and applied to model the donor-acceptor distance in single-molecule fluorescence experiments [27,61] in enzymes. Two-point correlation functions cannot distinguish between CTRWs and other dynamical models (e.g., the Gaussian process [27,62]). Systems with nonexponential correlations form universality classes [7,23]: different microscopic models under certain general conditions predict the same two-point correlation functions but are expected to have different multipoint correlation functions that could be measured by the nonlinear response [63,64]. Barsegov and Mukamel have used the FFPE to investigate the three-point correlation function for NPs [26]. Nonlinear optical spectroscopy is commonly used to distinguish between models that have the same two-point correlations (linear response) [62]. We demonstrate the capacity of multipoint correlation functions to distinguish between CTRWs and the Gaussian models of anomalous relaxation.

Green's functions of the GME, FFPE, and other types of non-Markovian descriptions of CTRWs cannot be directly used for calculating multipoint probabilities, as these may not be factorized into two-point Green's functions. We shall construct a recursive algorithm for multipoint functions based on densities of just arriving particles [2], which allows us to compute correlation functions in the frequency domain directly. An alternative stategy would be to use Markovian approaches (the SLE or ADME), which would involve representing age by additional variables, a larger matrix problem must then be solved.

Stationary CTRW ensembles with broad WTDs are defined in Sec. II. The CTRW in an external potential is calculated in Sec. III. A general algorithm for computing multipoint correlation functions for CTRWs is presented in Sec. IV. Applications are made in Sec. V to three-point correlation functions, where the CTRW is compared with a Gaussian process.

II. STATIONARY CTRW ENSEMBLES WITH ANOMALOUS RELAXATION

We consider a particle moving stochastically on a lattice with points x (time is continuous, space is discrete). We define the transition probability T_{xy} for the jump from y to x as

$$p(x;i+1)=\sum_y T_{xy}p(y;i), \tag{1}$$

where $p(x;i)$ is the probability to be at x after the ith jump and $\Sigma_x T_{xy}=1$ ($T_{xx}=0$, as a jump necessarily implies a change of position). The CTRW is defined by introducing the waiting-time probability distribution for the jump, $\psi(t)$, normalized as $\int_0^\infty \psi(t)dt=1$. The process is described by the matrix of jump rates (we denote matrices by a caret)

$$\hat{\Psi}_{xy}(t)\equiv \psi(t)\hat{T}_{xy}, \tag{2}$$

and by specifying the initial conditions. The probability density to find the particle at time τ_0 at x is $\rho_x(\tau_0)$, and the WTD $\psi'(t)$ for the first jump after τ_0 may be different from $\psi(t)$.

The survival probability $\phi(t)$ that no jump had occurred prior to t is connected to the waiting-time distribution:

$$\phi(t)=\int_t^\infty \psi(t')dt'. \tag{3}$$

In Laplace space Eq. (3) reads

$$\phi(s)=\frac{1-\psi(s)}{s}. \tag{4}$$

We further introduce the matrix of survival probabilities

$$\hat{\Phi}_{xy}(t)=\phi(t)\delta_{xy}. \tag{5}$$

We define the probability densities $\eta_x(\tau)$ that a jump occurs to x precisely at time τ. It follows from these definitions that

$$\eta_x(\tau)=\int_{\tau_0}^{\tau}\sum_y \hat{\Psi}_{xy}(\tau-\tau')\eta_y(\tau')d\tau'+\sum_y \hat{\Psi}'_{xy}(\tau-\tau_0)\rho_y(\tau_0). \tag{6}$$

The probability $\rho_x(\tau)$ to find the particle at time τ in a particular state is obtained by multiplying η by the survival probability $\phi(t)$ (that no jump had occurred for time t) and integrating over the time of the last jump,

$$\rho_x(\tau) = \phi'(\tau - \tau_0)\rho_x(\tau_0) + \int_{\tau_0}^{\tau} \phi(\tau - \tau')\eta_x(\tau')d\tau'. \quad (7)$$

The evolution of the system is calculated by solving the coupled Eqs. (6) and (7).

The solution to Eqs. (4), (6), and (7) is given in terms of the Green's function $\hat{\mathcal{G}}$,

$$\rho_x(\tau) = \sum_y \hat{\mathcal{G}}_{xy}(\tau, \tau_0)\rho_y(\tau_0). \quad (8)$$

In Laplace space

$$\hat{\mathcal{G}}(s) = \int_{\tau_0}^{\infty} e^{-s(\tau_1 - \tau_0)}\hat{\mathcal{G}}(\tau_1, \tau_0)d\tau_1$$

the Green's function is given by [40]

$$\hat{\mathcal{G}}(s) = \hat{\Phi}'(s) + \hat{\Phi}(s)[1 - \hat{\Psi}(s)]^{-1}\hat{\Psi}'(s). \quad (9)$$

Substituting Eq. (2) in Eq. (9) gives

$$\hat{\mathcal{G}}(s) = \frac{1 - \psi'(s) + [\psi'(s) - \psi(s)]\hat{T}}{s[\hat{1} - \hat{T}\psi(s)]}. \quad (10)$$

We consider two types of ensembles which differ by the WTD for the first jump ψ'.

(i) Assuming that all particles arrived at their sites exactly at the initial time we simply set $\psi'(t) = \psi(t)$. This defines a NP CTRW. The Green's function is given by Eq. (10) with $\psi'(s) = \psi(s)$.

(ii) For the process to be stationary (SP CTRW) we require the initial density ρ to be invariant to the jump event,

$$\hat{T}\rho(\tau_0) = \rho(\tau_0), \quad (11)$$

and ψ' must be connected to ψ by [54] [see Eq. (C9)]

$$\psi'(s) = \frac{\phi(s)}{\bar{t}} = \frac{1 - \psi(s)}{s\bar{t}}, \quad (12)$$

where $\bar{t}$ is the mean waiting time:

$$\bar{t} = \int_0^{\infty} \tau\psi(\tau)d\tau = -\left.\frac{d\psi(s)}{ds}\right|_{s=0}.$$

It follows from Eq. (12) that the stationary ensemble can only be constructed provided the WTD has a finite first moment; otherwise the system has a long time memory and never equilibrates. Correlations between temporal and spatial distributions do not build up in our model because Eq. (2) has a separable form. Substituting Eq. (12) in Eq.(10) we obtain

$$\hat{\mathcal{G}}(s) = \frac{1}{s} - \frac{1 - \psi(s)}{s^2\bar{t}}\left(\frac{\hat{1} - \hat{T}}{\hat{1} - \hat{T}\psi(s)}\right). \quad (13)$$

Any two-point quantity may be calculated using Eq. (13). A CTRW is generally a non-Markovian process, and knowledge of the two-point Green's function is not enough to calculate higher-order quantities. $\psi(t) = \bar{t}^{-1}\exp(-t/\bar{t})$ is an exception where the CTRW is equivalent to a Markovian master equation and higher-order quantities can be readily calculated.

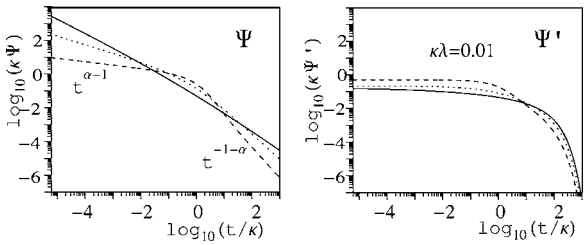

FIG. 1. Left panel: Anomalous WTD ψ_{AD} for $\alpha = 0.2$ (solid line), 0.5 (dotted line), and 0.8 (dash-dotted line) Right panel: Corresponding first-jump WTD ψ'_{TAD} for $\kappa\lambda = 0.01$.

We consider anomalous diffusion (AD) models characterized by algebraic waiting-time distributions with diverging first moment $\psi(t) \propto (t/\kappa)^{-(\alpha+1)}$ $(0 < \alpha < 1)$. In Laplace space we have $\psi(s) \propto 1 - (\kappa s)^{\alpha}$ for small s. We adopt the following form [49,60]:

$$\psi_{AD}(s) = \frac{1}{1 + (\kappa s)^{\alpha}}, \quad \phi_{AD}(s) = \frac{1}{s + \kappa^{-\alpha}s^{1-\alpha}}, \quad (14)$$

which in the time domain gives

$$\psi_{AD}(t) = -\frac{dE_{\alpha}(-(t/\kappa)^{\alpha})}{dt}, \quad \phi_{AD}(t) = E_{\alpha}(-(t/\kappa)^{\alpha}).$$

κ defines the time scale and E_{α} is the Mittag-Leffler function Eq. (A1) [65,66]. This function interpolates between the stretched-exponential form at short times $t \ll \kappa$

$$E_{\alpha}(-(t/\kappa)^{\alpha}) \approx \exp[-(t/\kappa)^{\alpha}/\Gamma(1 + \alpha)],$$

which gives

$$\psi_{AD}(t) = \frac{1}{\kappa^{\alpha}\Gamma(\alpha)}\frac{\exp[-(t/\kappa)^{\alpha}/\Gamma(1 + \alpha)]}{t^{1-\alpha}}, \quad (15)$$

and a power-law decay for $t \gg \kappa$

$$E_{\alpha}(-(t/\kappa)^{\alpha}) \approx \Gamma^{-1}(1 - \alpha)\left(\frac{\kappa}{t}\right)^{\alpha}, \quad \Gamma(s + 1) \equiv \int_0^{\infty} e^{-x}x^{s},$$

which yields

$$\psi_{AD}(t) = \frac{\alpha\kappa^{\alpha}}{\Gamma(1 - \alpha)}\frac{1}{t^{\alpha+1}}. \quad (16)$$

$\psi_{AD}(t)$ is displayed in the left panel of Fig. 1 for several values of α. The power law shows up as linear regions in the log-log plots; the short- and the long-time slopes become more different with increasing α [compare Eqs. (15) and (16)].

To define a SP we truncate the WTD to have a finite mean by adding a long-time cutoff parameter λ,

$$\psi_{TAD}(t) = [1 + (\kappa\lambda)^{\alpha}]e^{-\lambda t}\psi_{AD}(t)$$
$$= -[1 + (\kappa\lambda)^{\alpha}]e^{-\lambda t}\frac{dE_{\alpha}(-(t/\kappa)^{\alpha})}{dt}.$$

The algebraic decay $t^{-\alpha-1}$ on an intermediate time scale now

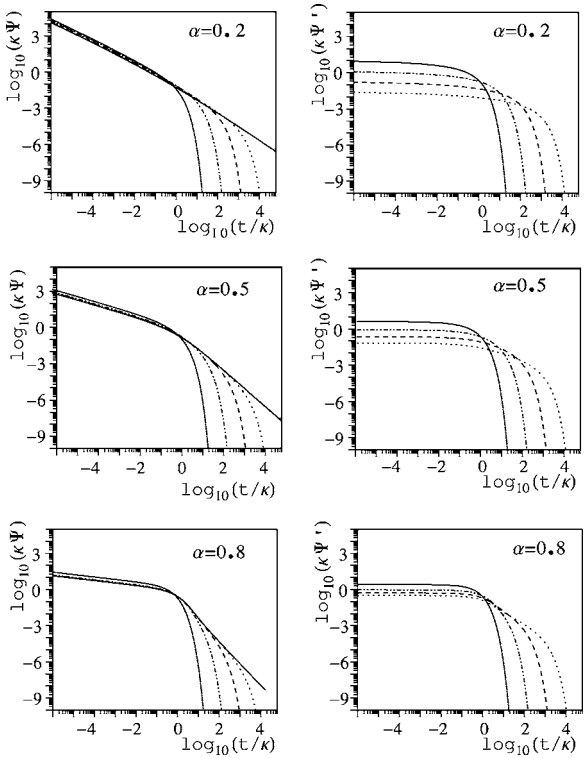

FIG. 2. Left panels: Truncated anomalous WTD ψ_{TAD} for $\alpha=0.2$ (top panel), 0.5 (central panel), and 0.8 (bottom panel) and with varying cutoff $\kappa\lambda=1$ (lower solid lines), 0.1 (dot-dashed lines), 0.01 (dashed lines), and 0.001 (dotted lines), and nontruncated anomalous WTD ψ_{AD} (i.e., $\lambda=0$) (upper solid lines). Right panels: Corresponding WTD for the first jumps ψ'_{TAD} except that $\lambda=0$ has no corresponding curve.

crosses over to an exponential decay for $\lambda t>1$ (Fig. 2, left column). In Laplace space this truncation shifts the s singularity by λ to the left in the complex plane,

$$\psi_{TAD}(s)=\frac{1+(\kappa\lambda)^{\alpha}}{1+[\kappa(s+\lambda)]^{\alpha}}. \tag{17}$$

The survival function is

$$\phi_{TAD}(s)=\frac{(s+\lambda)^{\alpha}-\lambda^{\alpha}}{s[\kappa^{-\alpha}+(s+\lambda)^{\alpha}]} \tag{18}$$

and the mean waiting time

$$\bar{t}=\frac{\alpha\lambda^{-1}}{1+(\kappa\lambda)^{-\alpha}}. \tag{19}$$

$\phi(t)$ is analytic for $s>-\lambda$, so it has exponential long-time decay given by

$$\phi_{TAD}(t)=\int_{t}^{\infty}\psi_{TAD}(t')dt'\approx\frac{\alpha\kappa^{\alpha}e^{-\lambda t}[1+(\kappa\lambda)^{\alpha}]}{\lambda t^{\alpha+1}\Gamma(1-\alpha)}.$$

For short times $(\lambda t)^{\alpha}\ll 1$ and $\kappa\lambda\ll 1$ the survival function is similar to that of the nontruncated model $\phi_{TAD}\approx\phi_{AD}$

$$\phi_{TAD}(t)\approx E_{\alpha}(-(t/\kappa)^{\alpha}). \tag{20}$$

Table I summarizes the typical time profiles for ψ_{TAD} and ϕ_{TAD}.

TABLE I. Typical time profiles for ψ_{TAD} and ϕ_{TAD}.

Time regime	Time scale	ψ_{TAD}	ϕ_{TAD}
Short	$t\ll\kappa$	$t^{\alpha-1}$	$e^{-(t/\kappa)^{\alpha}}$
Intermediate	$\kappa\ll t\ll\lambda^{-1}$	$t^{-\alpha-1}$	$t^{-\alpha}$
Long	$\lambda^{-1}\ll t$	$e^{-\lambda t}$	$e^{-\lambda t}$

For the stationary ensemble ψ' is obtained by substituting the survival function and the mean waiting time [Eq. (18)] in Eq. (12). The $\lambda\to 0$ limit is delicate since $\bar{t}$ diverges. The ratio $\kappa/\bar{t}$ shows the probability that the first jump will be observed on a similar time scale (κ) as the other jumps. It represents the fraction of fluctuating particles in the ensemble. Other particles are trapped—their first jump occurs on much longer time scales. This can be described in terms of equivalent multitrap models; see the discussion of Fig. 6 below. For small λ the fraction of fluctuating particles vanishes, the probability of early first jump is low, and the first jump appears on the λ^{-1} time scale.

ψ'_{TAD} is displayed in the right panel of Fig. 1 for $\kappa\lambda=0.01$ and for various α. The ψ'_{TAD} distribution is initially flat for $(t/\kappa)^{\alpha}\ll 1$ compared to the singular form of ψ_{AD} [Eq. (15)]. The stretched-exponential decay is followed by long-tailed algebraic decay for $\kappa\ll t\ll\lambda^{-1}$ if $(\kappa\lambda)^{\alpha}\ll 1$. This may best be seen for $\alpha=0.8$, which shows a linear region for $t/\kappa\in(1,50)$. The long-time decay is exponential.

ψ'_{TAD} is sensitive to the cutoff λ for any time scale, as demonstrated in Fig. 2, right column. For $t\ll\kappa$, ψ'_{TAD} is sensitive to λ due to the factor $1/\bar{t}$ in Eq. (12) which represents the fraction of fluctuating particles in the ensemble. ψ_{TAD} given in the left column does not show such sensitivity for $\kappa\lambda\ll 1$. The power-law decay appears as $(\kappa\lambda)^{\alpha}$ is decreased, best shown in the lower right panel $\psi'_{TAD}\sim t^{-\alpha}$ and $\psi_{AD}\sim t^{-\alpha-1}$. At long times, both ψ_{TAD} and ψ'_{TAD} decay exponentialy.

III. TWO-POINT CORRELATION FUNCTIONS FOR ANOMALOUS DIFFUSION IN AN EXTERNAL POTENTIAL

Diffusion in a potential can be described as a biased CTRW in the continuous-space limit. An anomalous nonstationary CTRW was recently described by the fractional Fokker-Planck equation [7,59,60]. For non-Markovian processes multipoint joint probabilities may not be factorized in terms of two-point ones. Equations of motion for densities are limited to two-point quantities; multipoint correlation functions are obtained by a more complicated procedures (e.g., [26] for the FFPE). We therefore do not derive a differential equation for densities in this paper; instead, we calculate the multipoint correlation functions using recursion relations.

Following the steps used in the derivation of the FFPE [59] we assume that the particle undergoes a one-dimensional CTRW along x with a finite step length a and probabilities $A_{-}(x),A_{+}(x)$ to move to the left and to the right, respectively. These are related to the external potential $V(x)$

and temperature T, by the detailed balance condition

$$\frac{A_+(x)}{A_-(x+a)} = \exp - \left(\frac{V(x+a) - V(x)}{kT} \right) \approx 1 + \frac{aF(x)}{kT}$$

where $F(x) \equiv -\partial V(x)/\partial x$ is the force. Since $A_+ + A_- = 1$ and assuming a small step $aF(x)/4kT \ll 1$ we have

$$A_+(x) = 1/2 + \frac{aF(x)}{4kT}, \quad A_-(x) = 1/2 - \frac{aF(x)}{4kT},$$

where k is the Boltzmann constant. Equation (1) now reads

$$p(x;i+1) = A_+(x-a)p(x-a;i) + A_-(x+a)p(x+a;i). \tag{21}$$

To second order in a Eq. (21) gives

$$p(x;i+1) = \left(1 + \frac{a^2 \hat{\mathcal{L}}}{2} \right) p(x;i), \tag{22}$$

where $\hat{\mathcal{L}}$ is the Fokker-Planck operator

$$\hat{\mathcal{L}} = \left(\frac{\partial^2}{\partial x^2} - \frac{\partial}{\partial x} \frac{F(x)}{kT} \right).$$

The transition matrix Eq. (1) now becomes

$$\hat{T} = \left(1 + \frac{a^2 \hat{\mathcal{L}}}{2} \right). \tag{23}$$

By the central limit theorem, the mean squared displacement for free diffusion scales asymptotically linearly with time, $\langle [x(t) - x(0)]^2 \rangle = Dt$, where $D \equiv a^2/2\bar{t}$ is the diffusion constant. In the following simulations we parametrize the model in terms of the diffusion constant instead of the step size a.

The matrices $\hat{\mathcal{G}}$, $\hat{\Psi}$, and $\hat{\Phi}$ have an infinite dimensionality, corresponding to the continuous index x. Equation (8) reads

$$\rho_{x'}(\tau_1) = \int dx \, \hat{\mathcal{G}}_{x'x}(\tau_1, \tau_0) \rho_x(\tau_0).$$

The CTRW is defined in analogy with Eqs. (1)–(4), but the summations over states are replaced by integrations over the continuous variable. The density of jumps to x, $\eta_x(\tau)$ at time τ, is connected to densities at previous times through the continuous limit of Eq. (6):

$$\eta_x(\tau) = \int_{-\infty}^{\infty} dx' \int_{\tau_0}^{\tau_1} \hat{\Psi}_{xx'}(\tau - \tau') \eta_{x'}(\tau') d\tau' + \int_{-\infty}^{\infty} dx' \hat{\Psi}'_{xx'}(\tau - \tau_0) \rho_{x'}(\tau_0); \tag{24}$$

and the probability density $\rho(x,t)$ of finding a particle at time t in state x is connected by

$$\rho_x(\tau) = \int_{\tau_0}^{\tau} \phi(\tau - \tau') \eta_x(\tau') d\tau' + \phi'(\tau - \tau_0) \rho_x(\tau_0), \tag{25}$$

in analogy with Eq. (7).

The waiting-time matrix for diffusion in the potential [Eq. (2)] and the survival matrix Eq. (5) take the forms

$$\hat{\Psi}_{xy}(t) = \psi(t) \hat{T}_{xy}, \quad \hat{\Phi}_{xy}(t) = \phi(t) \delta(x-y). \tag{26}$$

Adopting operator notation, Eqs. (24), (25), and (26) are identical to the discrete-space Eqs. (2), (5), (6), and (7) except that matrix multiplications are replaced by integrations.

The two-point Green's function is given by combining Eq. (10) with the diffusion model Eq. (23):

$$\hat{\mathcal{G}}(s) = \frac{1}{s} \frac{[1 - \psi(s)] - D\bar{t}\hat{\mathcal{L}}[\psi(s) - \psi'(s)]}{[1 - \psi(s)] - D\bar{t}\hat{\mathcal{L}}\psi(s)}. \tag{27}$$

This may be calculated by expanding it in the eigenbasis of right eigenvectors

$$\mathcal{L}\varphi_n = -\varepsilon_n \varphi_n, \quad n = 0, 1, \ldots,$$

and the left eigenvectors

$$\varphi'_n(x')\mathcal{L} = -\varepsilon_n \varphi'_n(x')$$

of the Fokker-Planck operator. The Green's function Eq. (27) is given by

$$\hat{\mathcal{G}}_{x'x}(s) = \sum_n \frac{1}{s} \frac{[1 - \psi(s)] + D\bar{t}\varepsilon_n[\psi(s) - \psi'(s)]}{[1 - \psi(s)] + D\bar{t}\varepsilon_n \psi(s)} \varphi_n(x') \varphi'_n(x). \tag{28}$$

For a stationary ensemble [Eq. (12)] this gives

$$\hat{\mathcal{G}}^{SP}_{x'x}(s) = \frac{1}{s} \sum_{n=0}^{\infty} \left(1 - \frac{\varepsilon_n}{sD^{-1} + s\varepsilon_n \bar{t} \psi(s)/[1 - \psi(s)]} \right) \varphi_n(x') \varphi'_n(x). \tag{29}$$

The joint probability distribution $P(\tau_1 x_1, \tau_0 x_0)$ is

$$P(\tau_1 x_1, \tau_0 x_0) = \hat{\mathcal{G}}_{x_1 x_0}(\tau_1, \tau_0) \rho_{x_0}(\tau_0)$$

and with the SP Green's function Eq. (29) we have

$$P(s_1 x_1, x_0) = \left(\frac{\delta(x_1 - x_0)}{s_1} - \sum_{n=0}^{\infty} \frac{\varepsilon_n \varphi_n(x_1) \varphi'_n(x_0)}{s_1^2 D^{-1} + s_1^2 \varepsilon_n \bar{t} \psi(s_1)/[1 - \psi(s_1)]} \right) \times \rho_{x_0}(\tau_0).$$

Hereafter we consider the truncated anomalous diffusion (TAD) model [Eq. (17)] in a harmonic potential:

$$V(x) = \frac{1}{2} M \Omega^2 x^2, \quad F(x) = -M\Omega^2 x, \tag{30}$$

where M is the mass. For TAD [Eq. (17)], the Green's function is independent of κ. The independent parameters of the SP model are the ratio of the diffusion constant and the cutoff $\epsilon \equiv \sigma^2 \lambda / D$, where $\sigma^2 = kT/(M\Omega^2)$, and λ, which simply scales with time:

$$\hat{\mathcal{G}}(s/\lambda; 1, \epsilon) = \lambda \hat{\mathcal{G}}(s; \lambda, \epsilon),$$

$$\hat{\mathcal{G}}((\tau_1-\tau_0);\lambda,\epsilon)=\hat{\mathcal{G}}(\lambda(\tau_1-\tau_0);1,\epsilon).$$

The Green's function Eq. (29) is then

$$\hat{\mathcal{G}}^{SP}_{x'x}(s')=\sum_{n=0}\frac{1}{\lambda s'}\left(1-\frac{n}{s'\epsilon+\alpha s' n/[(s'+1)^{\alpha}-1]}\right)\times\frac{\exp(-x'^2/2\sigma^2)}{2^n\sqrt{2\pi}n!\,\sigma}H_n\left(\frac{x'}{\sigma\sqrt{2}}\right)H_n\left(\frac{x}{\sigma\sqrt{2}}\right), \quad (31)$$

where $s'\equiv s/\lambda$ and H_n is the nth-order Hermite polynomial [Eq. (D5)].

The NP Green's function is obtained by substituting Eqs. (14) and (D4) in Eq. (E3):

$$\hat{\mathcal{G}}^{NP}_{x'x}(s)=\sum_{n}\frac{1}{s+nD_{\alpha}s^{1-\alpha}/\sigma^2}\frac{\exp(-x'^2/2\sigma^2)}{2^n\sqrt{2\pi}n!\,\sigma}\times H_n\left(\frac{x'}{\sigma\sqrt{2}}\right)H_n\left(\frac{x}{\sigma\sqrt{2}}\right). \quad (32)$$

The SP and NP distributions are shown in the lower and upper panels panels, respectively, of Fig 3. The peak near the initial position [$x=0.0$ (left panels) or 0.5 (right panels)] is consistent with the picture of a CTRW with a broad WTD as a mixture of diffusing and trapped particles [37].

The two-point correlation function $C(\tau_1,\tau_0)=\langle x(\tau_1)x(\tau_0)\rangle$ for a CTRW in a harmonic potential is given by Eq. (D9). Knowledge of $C(\tau_1,\tau_0)$ is sufficient to construct the CTRW model. The predicted multipoint correlation functions may be used to test its validity. For technical details see the discussion below Eq. (D9). For a SP [Eq. (12)] and TAD [Eq. (17)] the two-point correlation function [Eq. (D9)] is

$$C(s')=\frac{\sigma^2}{\lambda s'}\left(1-\frac{1}{\epsilon s'+\alpha s'/[(s'+1)^{\alpha}-1]}\right). \quad (33)$$

At short times $(\lambda t)^{\alpha}\ll 1$ we set $s'\gg 1$ and get

$$C(s')\approx\frac{\sigma^2}{\lambda s'}\left(1-\frac{1}{\epsilon s'+\alpha s'^{(1-\alpha)}}\right),$$

which gives

$$C(\tau_1,\tau_0)\approx\sigma^2\left(1-\frac{1}{\epsilon}\int_{\tau_0}^{\tau_1}E_{\alpha}[\alpha(\lambda\tau)^{\alpha}/\epsilon]d(\lambda\tau)\right).$$

For $(\lambda\tau)^{\alpha}\ll\epsilon/\alpha$ we have $C(\tau_1,\tau_0)\approx\sigma^2e^{-D(\tau_1-\tau_0)}$.

The complex form of relaxation for intermediate time scales $\lambda^{-1}(\epsilon/\alpha)^{1/\alpha}\ll t\ll\lambda^{-1}$ is simplified for $\epsilon\to 0$,

$$C(s')\approx\frac{\sigma^2}{\lambda\alpha s'^2}[1+\alpha s'-(1+s')^{\alpha}],$$

which in the time domain gives

$$C(\tau_1,\tau_0)\approx\sigma^2\left(1+\frac{\lambda(\tau_1-\tau_0)}{\alpha}-\sum_{j=0}^{\infty}\binom{\alpha}{j}\frac{[\lambda(\tau_1-\tau_0)]^{1-\alpha+j}}{\alpha\Gamma(2+j-\alpha)}\right)$$

with the leading term $C(\tau_1,\tau_0)\approx\sigma^2\{1-[\lambda(\tau_1-\tau_0)]^{1-\alpha}/\alpha\Gamma(2-\alpha)\}$. This type of decay was recently reported for a two-state CTRW model with broad distributions truncated by a step-function cutoff [57].

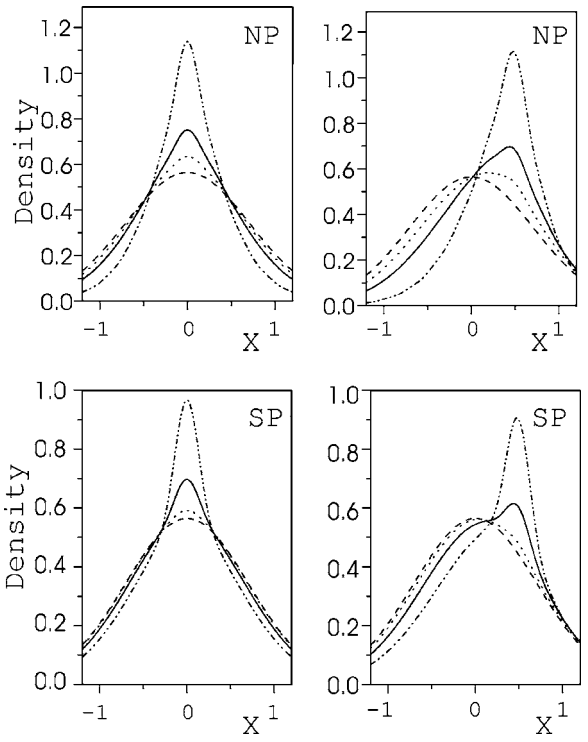

FIG. 3. Left panels: Probability distributions for CTRW relaxation from origin $x=0.0$. Upper panel: NP at times $(D_{\alpha}\sigma^2)^{1/\alpha}t=0.05$ (dot-dashed line), 1.5 (solid line), 20 (dotted line), and 500 (dashed line); parameters $\sigma=1/\sqrt{2}$, $\alpha=0.4$. Lower panel: SP at times $Dt/\sigma^2=1.3$ (dot-dashed line), 2.7 (solid line), 4.7 (dotted line), and 100 (dashed line); parameters $\sigma=1/\sqrt{2}$, $\lambda=0.5D/\sigma^2$, $\alpha=0.4$. Right panels: the same calculations but for a different initial state $x=\sigma/\sqrt{2}=0.5$.

For long times $\lambda t\gg 1$ we expect exponential decay. For $(\alpha/\epsilon)\leqslant 1$, the asymptotic decay rate is $\lambda[-1+(1-\alpha/\epsilon)^{1/\alpha}]$ [a pole in the complex plane for Eq. (33)]. For $(\alpha/\epsilon)>1$, the asymptotic decay rate is λ [a cut in the complex plane for Eq. (33)].

$C(t,0)$ is displayed vs $\log_{10}(t)$ in Fig. 4 for $\alpha=0.4$, and various values of ϵ (upper panel). $\ln[-\ln C(t,0)]$ vs $\log_{10}(t)$ plots show a stretched exponential $e^{-t^{\varphi}}$ as straight lines (central panel). In the lower panel the linearity of these plots is shown by the slope $\varphi\equiv d\ln[-\ln C(t)]/d\ln t$ for the curves of the central panel.

While normal relaxation $C(t,0)\approx e^{-Dt}$ is observed for $\epsilon\gg 1$, subexponential relaxation shows up as ϵ is decreased (i.e., longer cutoff) at intermediate time scales. The stretched-exponential form agrees with our model in this most interesting intermediate regime. Note that for $\epsilon\to 0$ the correlation function is controlled by λ over both intermediate and long time scales (the dotted $\epsilon=0.01$ and the solid $\epsilon=0.001$ lines are similar) and the diffusion constant is relevant only for very short times $t\ll\epsilon\lambda^{-1}$, in contrast to ordinary diffusion, which is controlled by D at all times.

In Fig. 5 we display the same quantities as in Fig. 4 for a fixed $\epsilon=0.001$ and various α. The stretched-exponential form is most clearly seen as α is decreased. The stretching parameter φ decreases with α for $\lambda^{-1}(\epsilon/\alpha)^{1/\alpha}\ll t$. This is in contrast to the correlation function for the NP [60]

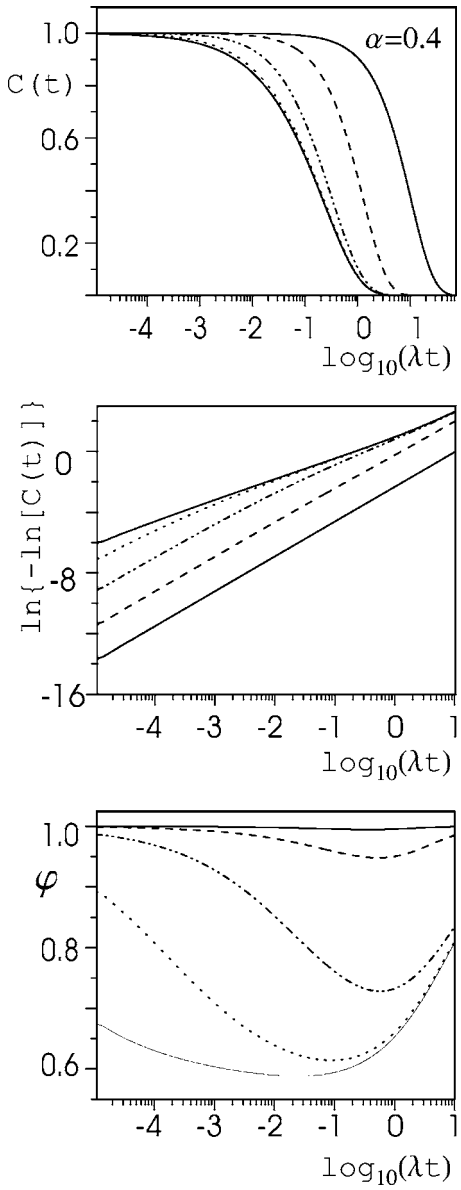

FIG. 4. Top panel: The two-point correlation function $C(t,0)$ vs $\log_{10}(\lambda t)$ for SP with $\alpha=0.4$ and various $\epsilon=10$ (upper solid line), 1 (dashed line) 0.1 (dash-dotted line), 0.01 (dotted line), and 0.001 (lower solid line). Central panel: $\ln\{\ln[-C(t,0)]\}$ vs $\log_{10}(\lambda t)$. Bottom panel: $\varphi = d\ln\{-\ln[C(t,0)]\}/d\ln t$ vs $\log_{10}(\lambda t)$.

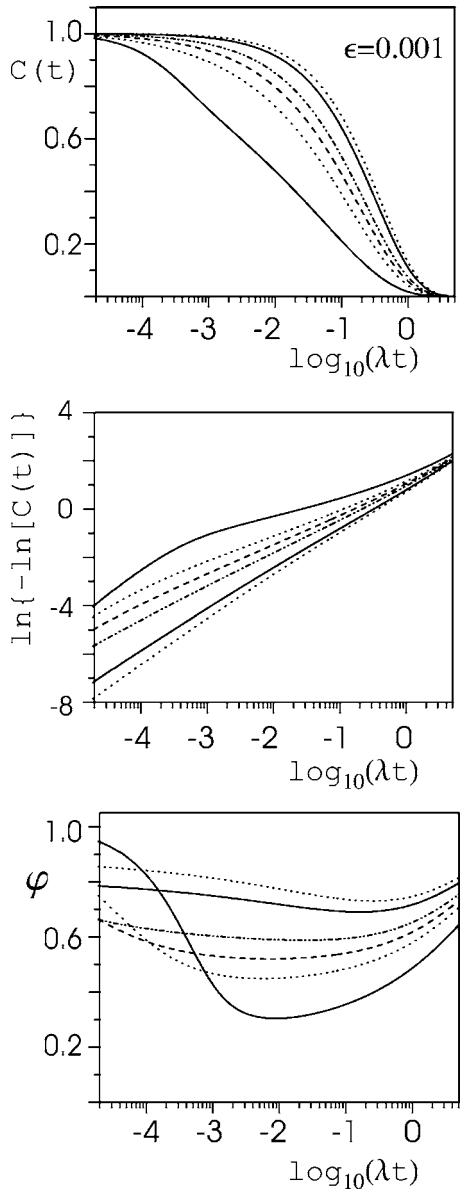

FIG. 5. Top panel: The two-point correlation function $C(t,0)$ vs $\log_{10}(\lambda t)$ for SP with $\epsilon=0.001$ and various $\alpha=0.1$ (upper dotted line), 0.2 (upper solid line), 0.4 (dot-dashed line), 0.5 (dashed line), 0.6 (lower dotted line), and 0.8 (lower solid line). Central panel: $\ln\{\ln[-C(t,0)]\}$ vs $\log_{10}(\lambda t)$. Bottom panel: $\varphi = d\ln\{-\ln[C(t,0)]\}/d\ln t$ vs $\log_{10}(\lambda t)$.

$$C(\tau,0) = \sigma^2 E_\alpha(-D_\alpha \tau^\alpha) \tag{34}$$

which decays more slowly with decreasing α.

We next consider the correlation function of

$$f(x) \equiv \exp \beta\hat{x}. \tag{35}$$

This form serves as the generating function for any function of x (x^p is obtained by differentiation with respect to β and setting $\beta=0$).

We focus on

$$B^{(2)}(\tau_1,\tau_0) \equiv \langle \delta f(\tau_1)\delta f(\tau_0)\rangle \tag{36}$$

where $\delta f \equiv f - \langle f\rangle$. For our harmonic model Eq. (30) we have

$$\langle f(x)\rangle = \exp[(\beta\sigma)^2/2]. \tag{37}$$

$B^{(2)}$ is calculated in Appendix D. By combining Eq. (D12) with the TAD model Eq. (17) we finally obtain

$$B^{(2)}_{SP}(s') = \lambda^{-1}\exp(\beta\sigma)^2 \sum_{n=1}^{\infty} \frac{(\beta\sigma)^{2n}}{n!} \times \frac{1}{s'}\left(1 - \frac{1}{s'\epsilon/n + \alpha s'/[(s'+1)^\alpha - 1]}\right), \tag{38}$$

which is different from the NP [60]

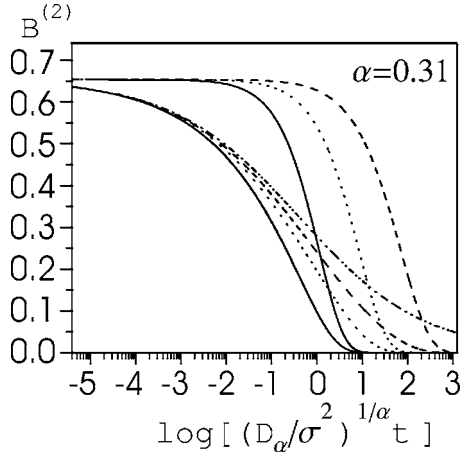

FIG. 6. $B^{(2)}(t,0)$ for NP CTRW (lower curves) with varying λ and comparison to SPCTRW (upper curves) of the same systems. Parameters: $D_\alpha/\sigma^2=2.19$, $\kappa=10^{-5}$, $\alpha=0.31$, $(\beta\sigma)^2=0.372$, $(D_\alpha/\sigma^2)^{1/\alpha}/\lambda=2.245$ (solid line), 22.45 (dotted line), 224.5 (dashed line), and 5.585 (dot-dashed line); $\lambda=0$ (dot-dashed line, the nonstationary model only).

$$B_{NP}^{(2)}(s)=\exp(\beta\sigma)^2\sum_{n=1}^{\infty}\frac{(\beta\sigma)^{2n}}{n!}\frac{1}{s+nD_\alpha s/\sigma^2[(s+\lambda)^\alpha-\lambda^\alpha]}. \tag{39}$$

In Fig. 6 we compare $B_{SP}^{(2)}$ and $B_{NP}^{(2)}$. The different role of the cutoff is illustrated by varying λ for fixed a,κ of the NP. The NP correlation function approaches the anomalous solution of [7] for $\lambda\to 0$; λ controls the time scale where the Mittag-Leffler behavior crosses over to exponential (Fig 1). In contrast, the SP correlation function is controlled by λ over the entire relaxation time.

The qualitatively different behavior of stationary and nonstationary ensembles can be rationalized by a multitrap picture, where λ controls the allowed trap depths [37]. The NP describes the relaxation to equilibrium of just arrived particles. The allowed trap depth cannot be observed for times earlier than λ^{-1}. In contrast, a substantial fraction of particles is trapped at equilibrium, and the fraction of mobile particles as well as the escape time from the trap are related to λ. For very small λ and at equilibrium, all particles are deeply trapped; the waiting time for the first jump becomes infinitely longer than the time scale for the WTD of other jumps κ.

For comparison we consider a Gaussian process (Brownian oscillator) with the same two-point correlation function $C(\tau_1,\tau_0)$ as the SP [Eq. (33)]. Using the second-order cumulant expansion we obtain [62,67]

$$B_{GP}^{(2)}(\tau_1,\tau_0)=e^{\beta^2\sigma^2}(e^{\beta^2 C(\tau_1,\tau_0)}-1). \tag{40}$$

In Fig. 7 we compare $B_{GP}^{(2)}$ [Eqs. (33) and (40)] and $B_{SP}^{(2)}$ [Eq. (38)]. The left upper panel shows the SP for $\alpha=0.4$, $\epsilon=1$. The right column shows the GP. For small $\beta\sigma<1$ the dominant contribution comes from the first Fokker-Planck eigenmode, which is described by $C(\tau_1,\tau_2)$; the GP and SP models then coincide. Increasing $\beta\sigma$ highlights the role of

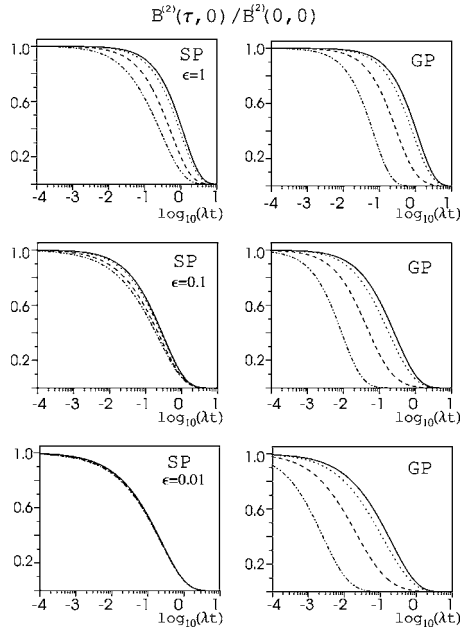

FIG. 7. Left panels: $B_{SP}^{(2)}(\tau,0)/B_{SP}^{(2)}(0,0)$ for $\alpha=0.4$ and various $(\beta\sigma)=0.5$ (solid lines), 1.0 (dotted lines), 2.0 (dashed lines), and 4.0 (dot-dashed lines). $\epsilon=1$, (top panel), 0.1 (central panel), and 0.01 (bottom panel). Right panels: Corresponding curves $B_{GP}^{(2)}(\tau,0)/B_{GP}^{(2)}(0,0)$ for GP with $C_{GP}(\tau,0)=C_{SP}(\tau,0)$.

higher modes, and faster relaxation is observed. The SP relaxation is not controlled by the diffusion constant for $\epsilon\to 0$, so with decreasing $\epsilon=0.1$ (0.01) in the central (lower) panels the changes with $\beta\sigma$ are less pronounced. GP decay (right panels) is significantly faster with increasing $\beta\sigma$, which is seen for all ϵ.

Figure 8 displays $B_{SP}^{(2)}$ (left panels) and the corresponding $B_{GP}^{(2)}$ for $\epsilon=0.1$, various $\beta\sigma$, and for $\alpha=0.2$ (upper panel), 0.4 (middle panel), and 0.6 (lower panel). The relaxation of the GP model is faster compared to the SP in all cases. With decreasing α the differences between SP and GP are stronger; with $\alpha=1$ we approach normal relaxation.

IV. MULTIPOINT CORRELATION FUNCTIONS

We consider a sequence of $n+1$ measurements of x carried out at times $\tau_0,\tau_1,\ldots,\tau_n$ yielding the values $x_0,x_1,\ldots,x_n$. The multipoint correlation function of an arbitrary function of x, $f(x)$, is defined as

$$C^{(n+1)}(\tau_n,\ldots,\tau_0)\equiv\langle f(x_n)\cdots f(x_0)\rangle, \tag{41}$$

where $\langle\ \rangle$ denotes averaging over realizations of the random walk.

The joint probability distribution function (PDF) is similarly defined by

$$P^{(n+1)}(\tau_n y_n,\ldots,\tau_1 y_1,\tau_0 y_0)\equiv\langle\delta(y_n-x_n)\cdots\delta(y_0-x_0)\rangle, \tag{42}$$

and the two are connected by

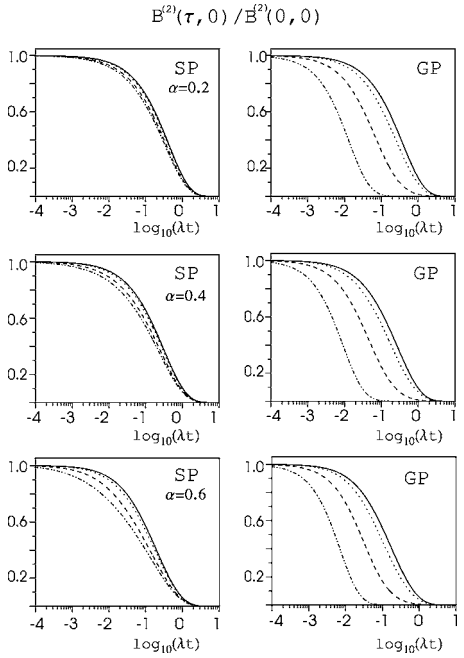

FIG. 8. Left panels: $B^{(2)}_{SP}(\tau,0)/B^{(2)}_{SP}(0,0)$ for SP, $\epsilon=0.1$, and various $(\beta\sigma)=0.5$ (solid lines), 1.0 (dotted lines), 2.0 (dashed lines), and 4.0 (dot-dashed lines). Various $\alpha=0.2$ (top panel), 0.4 (central panel), and 0.6 (bottom panel). Right panels: Corresponding curves $B^{(2)}_{GP}(\tau,0)/B^{(2)}_{GP}(0,0)$ for GP with $C_{GP}(\tau,0)=C_{SP}(\tau,0)$.

$$C^{(n+1)}(\tau_n,\ldots,\tau_0) = \sum_{y_n}\cdots\sum_{y_0} f(y_n)\cdots f(y_0)P(\tau_n y_n,\ldots,\tau_1 y_1,\tau_0 y_0). \tag{43}$$

Correlation functions are given by moments of the PDF and carry less information. For instance, one cannot distinguish between the contributions to the n-point correlation function from trajectories that visit the same states but in a permuted order in time.

To calculate the PDF Eq. (42) we introduce some auxiliary quantities. We first define a projection to state $|x_k\rangle,\hat{\Theta}(x_k)\equiv|x_k\rangle\langle x_k|$. Predicting the future evolution of the system requires the present distribution function of x as well as the distribution of the prior (last) jump. The density of just arrived particles η [Eq. (6)] is most useful in studies of two-point correlations. For multipoint correlation functions and fixed results of previous measurement at times $\tau_0,\ldots,\tau_{k-1}$ we focus on paths with a jump at some fixed later time $\tau_k > \tau_{k-1}$.

We consider a particle that starts at time τ_0 in state x_0 (τ_0 is the onset of the random walk; Appendix E shows how the Ψ' is changed from Ψ if the NP started in some earlier time) and denote $\hat{R}^{(k)}_{x_k x_0}(\tau_k,\tau_0;\tau_{k-1}x_{k-1},\ldots,\tau_1 x_1)$ the probability to find it in time τ_1 at state x_1, … at time τ_{k-1} in x_{k-1} and that a jump had occurred to state x_k exactly at time τ_k (any number of jumps between τ_{k-1} and τ_k is allowed). We further define a second auxiliary matrix $\hat{\Xi}^{(k)}_{x_k x_0}(\tau_k,\tau_0;\tau_{k-1}x_{k-1},\ldots,\tau_1 x_1)$, the probability to find a particle that starts at time τ_0 at x_0 at time τ_1 at x_1,…, at time τ_{k-1} at x_{k-1}, that the *first* jump after τ_{k-1} occurs exactly at time τ_k to state x_k, and that no other jump occurs in the τ_k,τ_{k-1} period. (See Fig. 9.)

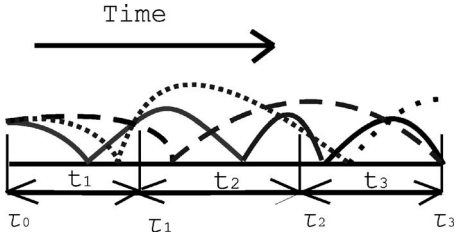

FIG. 9. Path contributions to $\hat{R}^{(3)}$ and $\hat{\Xi}^{(3)}$ in multistate system. Jumps (change of state) occur when the curves touch the time axis. The system is in state x_0,x_1,x_2,x_3 at times $\tau_0,\tau_1,\tau_2,\tau_3$, respectively; t_1,t_2,t_3 are the intervals between measurements. Both dashed and solid paths contribute to $\hat{R}^{(3)}_{x_3,x_0}(\tau_3,\tau_0;\tau_2x_2,\tau_1x_1)$ as they jump at τ_3. Only the dashed path contributes to $\hat{\Xi}^{(3)}_{x_3,x_0}(\tau_3,\tau_0;\tau_2x_2,\tau_1x_1)$ where the jump at τ_3 is the very first after τ_2. The dotted path contributes neither to $\hat{R}^{(3)}_{x_3,x_0}(\tau_3,\tau_0;\tau_2x_2,\tau_1x_1)$ nor to $\hat{\Xi}^{(3)}_{x_3,x_0}(\tau_3,\tau_0;\tau_2x_2,\tau_1x_1)$, as it has no jump at τ_3.

$\hat{R}^{(k)}$ may be constructed from its values at earlier times. The jump preceding τ_k could occur either during the (τ_{k-1},τ_k) interval or in any of the previous intervals. This leads to the following relation between $\hat{R}^{(k)}$ and $\hat{\Xi}^{(k)}$:

$$\hat{R}^{(k)}(\tau_k,\tau_0;\tau_{k-1}x_{k-1},\ldots,\tau_1x_1) = \hat{\Xi}^{(k)}(\tau_k,\tau_0;\tau_{k-1}x_{k-1},\ldots,\tau_1x_1) + \int_{\tau_{k-1}}^{\tau_k} d\tau'\hat{\Psi}(\tau_k-\tau')\hat{R}^{(k)}(\tau',\tau_0;\tau_{k-1}x_{k-1},\ldots,\tau_1x_1). \tag{44}$$

The first term accounts for the paths where the jump before the last at τ_k occurred prior to τ_{k-1}. The second term is the contribution of the paths where the preceding jump occurred at $\tau_{k-1}<\tau'<\tau_k$. The probability for a jump at $\tau'[\hat{R}^{(k)}\times(\tau',\tau_0;\ldots)]$ is multiplied by the probability $\Psi(\tau_k-\tau')$ to have the next jump τ_k.

$\hat{\Xi}^{(k)}$ is obtained by summing over all possible realizations of the previous jump

$$\hat{\Xi}^{(k)}(\tau_k,\tau_0;\tau_{k-1}x_{k-1},\ldots,\tau_1x_1) = \hat{\Psi}'(\tau_k-\tau_0)\prod_{j=1}^{k-1}\hat{\Theta}^{(j)}(x_j) + \sum_{j=1}^{k-1}\int_{\tau_{j-1}}^{\tau_j}\hat{\Psi}(\tau_k-\tau') \times\prod_{q=j}^{k-1}\hat{\Theta}(x_q)\hat{R}^{(j)}(\tau',\tau_0;\tau_{j-1}x_{j-1},\ldots,\tau_1x_1)d\tau'. \tag{45}$$

The first term represents paths with no jump between τ_0 and τ_k. Contributions of paths where the jump before the last at τ_k occurs in the jth time interval (τ_{j-1},τ_j) are summed in the second term of Eq. (45). These are given by the probability to have a jump at prior time τ', the waiting-time function to have a next jump after a $\tau_k-\tau'$ interval and projected to the states observed at times $\tau_j,\ldots,\tau_{k-1}$ between these two jumps.

Equations (44) and (45) form a closed system for $\hat{R}^{(1)},\ldots,\hat{R}^{(k)}$ and $\hat{\Xi}^{(1)},\ldots,\hat{\Xi}^{(k)}$. They may be recursively solved in Laplace space order by order for $k=1$, then $k=2$, etc. (see Appendix C).

Having calculated $\hat{R}^{(k)}$ we can obtain the Green's function, $\hat{\mathcal{G}}^{(n+1)}_{x_n,x_0}(\tau_n,\tau_0;\tau_{n-1}x_{n-1},\ldots,\tau_1x_1)$: the probability for the particle which starts at τ_0 at x_0 to go through the path $\tau_1x_1,\ldots,\tau_nx_n$. $\hat{\mathcal{G}}$ is given by multiplying $\hat{R}^{(k)}$ by the survival probability from the last jump $\hat{\Phi}$ and integrating over the time of the last jump:

$$\hat{\mathcal{G}}^{(n+1)}(\tau_n,\tau_0;\tau_{n-1}x_{n-1},\ldots,\tau_1x_1) = \hat{\Phi}(\tau_n-\tau_0)\prod_{q=1}^{n}\hat{\Theta}(x_q)+\sum_{k=1}^{n}\int_{\tau_{k-1}}^{\tau_k}\hat{\Phi}(\tau_n-\tau')\prod_{q=k}^{n}\hat{\Theta}(x_q) \times\hat{R}^{(k)}(\tau',\tau_0,t_{k-1},x_{k-1},\ldots,t_1x_1)d\tau'. \quad (46)$$

The PDF for a particle to be at τ_0 at x_0, …, and at τ_n at x_n is finally given by

$$P(\tau_nx_n,\ldots,\tau_0x_0)=\hat{\mathcal{G}}^{(n+1)}_{x_n,x_0}(\tau_n,\tau_0;\tau_{n-1}x_{n-1},\ldots,\tau_1x_1)\rho_{x_0}(\tau_0). \quad (47)$$

In summary our algorithm for computing the multipoint correlation function consists of the following steps. We first apply Eqs. (44) and (45) to calculate the auxiliary matrices $\hat{R}^{(1)},\hat{\Xi}^{(1)},\ldots,\hat{R}^{(n)},\hat{\Xi}^{(k)}$, which are then substituted into Eq. (46) to obtain the Green's function $\hat{\mathcal{G}}^{(n+1)}$. The PDFs are finally calculated using Eq. (47). For two-point quantities this algorithm coincides with Eqs. (9) and (13).

The general form of the three-point PDF is obtained in Appendix C by solving Eqs. (44), (45), and (46) and is given by

$$\begin{aligned}P^{(3)}(s_2x_2,s_1x_1,x_0) &= \frac{1}{(s_1-s_2)}\left(\frac{1-\psi'(s_2)}{s_2}-\frac{1-\psi'(s_1)}{s_1}\right)\delta_{x_2x_1}\delta_{x_1x_0}\rho_{x_0}(\tau_0)\\ &+\frac{[1-\psi(s_2)][\psi(s_2)-\psi(s_1)]\psi'(s_1)}{s_2(s_1-s_2)}\left[\frac{\hat{T}}{1-\hat{T}\psi(s_2)}\right]_{x_2,x_1}\left[\frac{\hat{T}}{1-\hat{T}\psi(s_1)}\right]_{x_1,x_0}\rho_{x_0}(\tau_0)\\ &+\frac{[1-\psi(s_2)][\psi'(s_2)-\psi'(s_1)]}{s_2(s_1-s_2)}\left[\frac{\hat{T}}{1-\hat{T}\psi(s_2)}\right]_{x_2,x_1}\delta_{x_1x_0}\rho_{x_0}(\tau_0)\\ &+\delta_{x_2x_1}\psi'(s_1)\left(\frac{1-\psi(s_2)}{s_2(s_1-s_2)}-\frac{1-\psi(s_1)}{s_1(s_1-s_2)}\right)\left[\frac{\hat{T}}{1-\hat{T}\psi(s_1)}\right]_{x_1,x_0}\rho_{x_0}(\tau_0). \end{aligned} \quad (48)$$

For a SP Eq. (48) reduces to

$$\begin{aligned}P^{(3)}(s_2x_2,s_1x_1,x_0) &= \frac{\delta_{x_2x_1}\delta_{x_1x_0}}{s_1s_2}\rho_{x_0}(\tau_0)-\delta_{x_1x_0}\frac{1-\psi(s_2)}{s_1s_2^2\bar{t}}\left[\frac{\hat{1}-\hat{T}}{\hat{1}-\hat{T}\psi(s_2)}\right]_{x_2,x_1}\rho_{x_0}(\tau_0)-\delta_{x_2x_1}\frac{1-\psi(s_1)}{s_2s_1^2\bar{t}}\left[\frac{\hat{1}-\hat{T}}{\hat{1}-\hat{T}\psi(s_1)}\right]_{x_1,x_0}\rho_{x_0}(\tau_0)\\ &+\frac{\psi(s_2)-\psi(s_1)}{(s_1-s_2)s_1s_2\bar{t}}\left[\frac{\hat{1}-\hat{T}}{\hat{1}-\hat{T}\psi(s_2)}\right]_{x_2,x_1}\left[\frac{\hat{1}-\hat{T}}{\hat{1}-\hat{T}\psi(s_1)}\right]_{x_1,x_0}\rho_{x_0}(\tau_0). \end{aligned} \quad (49)$$

The three-point correlation function may be calculated using Eqs. (43) and (49).

V. THREE-POINT CORRELATION FUNCTIONS

We consider the three-point correlation functions of $\delta f\equiv f-\langle f\rangle$ where $f(x)=\exp\beta x$ for the diffusion model in a harmonic potential [Eqs. (23) and (30)]:

$$B^{(3)}(\tau_2,\tau_1,\tau_0)\equiv\langle\delta f(\tau_2)\delta f(\tau_1)\delta f(\tau_0)\rangle. \quad (50)$$

This is given by

$$B^{(3)}(\tau_2,\tau_1,\tau_0)=\mathcal{B}^{(3)}(\tau_2,\tau_1,\tau_0)-[B^{(2)}(\tau_1,\tau_0)+B^{(2)}(\tau_2,\tau_1)+B^{(2)}(\tau_2,\tau_0)]\langle f\rangle-\langle f\rangle^3, \quad (51)$$

where $\mathcal{B}^{(3)}(\tau_2,\tau_1,\tau_0)\equiv\langle f(\tau_2)f(\tau_1)f(\tau_0)\rangle$.

We compare the SP and GP stationary models for anomalous diffusion introduced in the previous sections. For the SP [Eq. (12)] $\mathcal{B}^{(3)}$ is given by Eq. (D14), which for the TAD model [Eq. (17)] gives

$$B^{(3)}_{SP}(s'_2,s'_1)=\lambda^{-2}\exp[3(\beta\sigma)^2/2]\sum_{k=0}^{\infty}\sum_{m=0}^{\infty}\sum_{j=0}^{\infty}\frac{(\beta\sigma)^{2(m+k+j)}}{m!\,k!\,j!}\left(\frac{1}{s'_1s'_2}-\frac{1}{s'_1s'^2_2\left(\frac{\alpha}{(s'_2+1)^\alpha-1}+\frac{\epsilon}{(j+k)}\right)}-\frac{1}{s'_2s'^2_1\left(\frac{\alpha}{(s'_1+1)^\alpha-1}+\frac{\epsilon}{(j+m)}\right)}\right.$$
$$\left.+\frac{(s'_2+1)^\alpha-(s'_1+1)^\alpha}{\alpha(s'_1-s'_2)s'_1s'_2\left(1+\frac{\epsilon[(s'_2+1)^\alpha-1]}{\alpha(j+k)}\right)\left(1+\frac{\epsilon[(s'_1+1)^\alpha-1]}{\alpha(j+m)}\right)}\right) \tag{52}$$

where $s'\equiv s/\lambda$. $B^{(3)}(\tau_2,\tau_1,\tau_0)$ is obtained by substituting Eqs. (37), (38), and (52) in Eq. (51).

Note that Eq. (52) obeys $B^{(3)}(s_b,s_a)=B^{(3)}(s_a,s_b)$. This relation follows from the time-reversal and time-translational invariance of stationary ensembles [27]:

$$B^{(3)}(t_a+t_b,t_b,0)=B^{(3)}(t_b+t_a,t_a,0). \tag{53}$$

For comparison, the three-point correlation function for a GP is obtained from the second-order cumulant expansion [62,67]

$$B^{(3)}_{GP}(\tau_2,\tau_1,\tau_0)=e^{3(\beta\sigma)^2/2}(e^{\beta^2C(\tau_1,\tau_0)+\beta^2C(\tau_2,\tau_1)+\beta^2C(\tau_2,\tau_0)}-e^{\beta^2C(\tau_1,\tau_0)}-e^{\beta^2C(\tau_2,\tau_1)}-e^{\beta^2C(\tau_2,\tau_0)}+2) \tag{54}$$

where $C_{GP}(\tau_1,\tau_0)=C_{SP}(\tau_1,\tau_0)$ is taken to be identical for the GP and SP [Eq.(33)].

The three-point SP and GP correlation functions are compared in Figs. 10 and 11 for $\alpha=0.8$, $\epsilon=10^{-5}$, and $(\beta\sigma)^2=0.372$. [For $\beta\sigma<1$ $B^{(2)}_{SP}\approx B^{(2)}_{GP}$ since both reduce to $C(t)$ as shown in Figs. 7 and 8.]

Contour plots of $B^{(3)}(t_2+t_1,t_1,0)$ displayed for several time decades show subexponential relaxation. Contours are linear for $B^{(3)}_{SP}(t_1+t_2,t_1,0)$ and curved for $B^{(3)}_{GP}(t_1+t_2,t_1,0)$. $B^{(3)}_{SP}(\tau_2,\tau_1,\tau_0)$ are insensitive to τ_1 and depend primarily on the $\tau_2-\tau_0$ interval. This is consistent with the picture that trapped particles make significant contributions to long-time correlations. GP relaxation is faster along the diagonal direction. Both GP and SP contours are symmetric along the diagonal. This is a consequence of Eq. (53). These figures demonstrate the capacity of higher-order correlations to distinguish between various dynamical models.

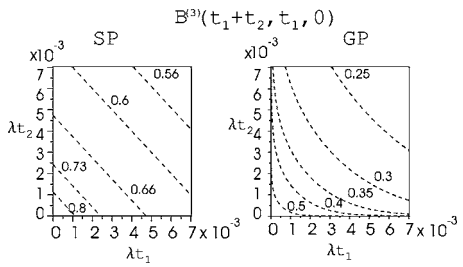

FIG. 10. Left: Contour plot for the three-point correlation function $B^{(3)}_{SP}(t_1+t_2,t_1,0)$ for SP with $\alpha=0.8$, $\epsilon=10^{-5}$, $(\beta\sigma)^2=0.372$. Right: Same plot for the Gaussian model $B^{(3)}_{GP}(t_1+t_2,t_1,0)$ with $C_{GP}(t,0)=C_{SP}(t,0)$.

Logarithmic scale plots of $B^{(3)}$ (Fig. 12) show that the GP contours (right panel) are not perpendicular to the time axis even when the time intervals t_1 and t_2 differ by four orders of magnitude. In comparison, the three-point correlation function for the SP (left panel) only changes when t_1,t_2 are comparable and both contribute to the t_1+t_2 time interval. This observation is equivalent to the straight vs curved contours in Figs. 10 and 11. The three-point correlation functions along the diagonal $t_1=t_2$ are compared in Fig. 13. The decay of the Gaussian model is significantly faster. This results from two factors. First, higher eigenmodes can contribute $[C^{(3)}\times(\tau_2,\tau_1,\tau_0)\equiv\langle x(\tau_2)x(\tau_1)x(\tau_0)\rangle=0]$ resulting in faster GP relaxation as pointed out in the discussion of Figs. 7 and 8. Second, as shown in Figs. 10 and 11, the diagonal decay $B^{(3)}_{GP}(2t,t,0)$ is significantly faster than $B^{(3)}_{GP}(2t,0,0)$.

In summary, we have computed multipoint correlation functions for continuous-time random walks with truncated anomalous WTD of stationary ensembles. Our model interpolates between normal and highly subexponential relaxation. Stretched-exponential relaxation has been observed for two-point correlation functions for the CTRW in a harmonic potential. This is similar to the short-time regime of nonstationary random walks commonly used in modeling of anomalous diffusion. However, anomalous relaxation of stationary random walks is controlled by the cutoff parameter. We have not observed the power-law decays (known from the NP) for the TAD model; however, these can also be modeled with stationary random walks by employing other forms of long-tailed waiting-time distributions as shown in Appendix B. We developed a general algorithm for calculating multipoint CTRW correlation functions. Significant differences in the three-point correlation function $B^{(3)}$ of $f(x)$ were found for the stationary CTRW and the Brownian oscillator model

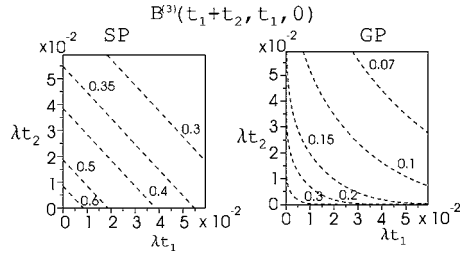

FIG. 11. Longer times for Fig. 10.

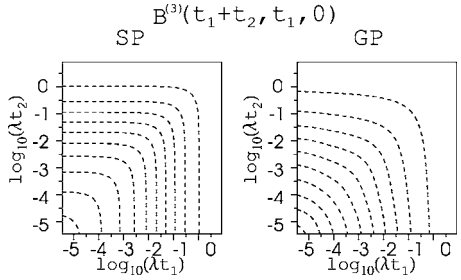

FIG. 12. Left panel: Contour plot on $\log_{10}$-$\log_{10}$ time scale for three-point correlation function $B^{(3)}_{SP}(t_1+t_2,t_1,0)$ for SP with $\alpha=0.8$, $\epsilon=10^{-5}$, $(\beta\sigma)^2=0.372$. (Dashed contours connect time points with equal correlations $B^{(3)}=0.02,0.15,0.3,0.45,0.6,0.75,0.9,1.05$.) Right panel: Similar plot for Gaussian model $B^{(3)}_{GP}\times(t_1+t_2,t_1,0)$ with $C_{GP}(t)=C_{SP}$. Three-point correlation function for CTRW and Brownian model with identical $C_{SP}(t,0)=C_{GP}(t,0)$ on logarithmic scale.

(Gaussian process) with identical two-point correlation functions C of x.

Equations (44)–(46) can be generalized to describe nonlinear optical response functions by including the dynamics of coherences in Liouville space. The non-Markovian stochastic Liouville equation [50] has been used for linear response (two-point correlation function). The present approach allows the calculation of a higher-order multipoint optical response. This extension will be made in the future.

ACKNOWLEDGMENTS

The support of the National Science Foundation (Grant No. CHE-0446555), NIRT (Grant No. EEC 0303389), the Air Force Office of Scientific Research (Grant No. FA 9550-04-10332), and the National Institute of Health (Grant No. GM59230-05) is gratefully acknowledged. We wish to thank to Dr. M. Shlesinger, and Professor J. Klafter for most valuable discussions.

APPENDIX A: ANALYTIC PROPERTIES OF NONINTEGER EXPONENTS IN THE COMPLEX PLANE

To find the noninteger exponent for Eq. (14) we note that since $\psi(s)^*=\psi(s^*)$, the cut in the complex plane must be on the real axis in the negative half plane. For $s>0$ ψ is analytic and further we assume positivity $\psi(t)\geqslant 0$ and normalization $\psi(s=0)=1$. Similar properties are assumed to hold for ϕ, $[1-\Psi(s)]^{-1}$.

Thus the exponents are defined $(z>0)$ as

$$(z+i\omega)^\alpha=(z^2+|\omega|^2)^{\alpha/2}\left[\cos\left(\alpha\arctan\frac{\omega}{z}\right)+i\sin\left(\alpha\arctan\frac{\omega}{z}\right)\right]$$

with $\arctan\in(-\pi/2;\pi/2)$.

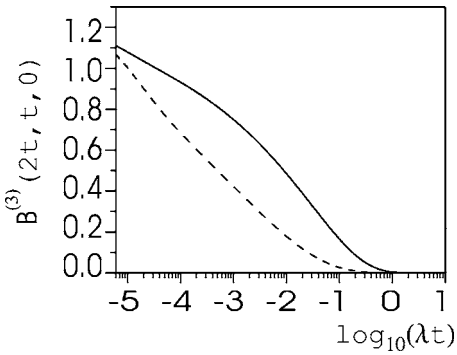

FIG. 13. Correlation function $B^{(3)}(2t,t,0)$ is compared for the SP (solid line) with parameters $\alpha=0.8$, $\epsilon=10^{-5}$, $(\beta\sigma)^2=0.372$ and the GP (dashed line) with $C_{SP}(t,0)=C_{GP}(t,0)$.

The Mittag-Leffler function is defined using reverse Laplace transform

$$E_\alpha(-t)\equiv\frac{1}{2\pi i}\int_{-i\infty}^{i\infty}dz\frac{e^z}{z+tz^{1-\alpha}} \tag{A1}$$

with series expansion

$$E_\alpha(-t)=\sum_{n=0}^{\infty}\frac{(-t)^n}{\Gamma(1+\alpha n)}.$$

The Mittag-Leffler function interpolates between the initial period $t\ll 1$ of exponential decay

$$E_\alpha(-t)\approx e^{-t/\Gamma(1+\alpha)}$$

and the power-law decay at long times $t\gg 1$

$$E_\alpha(-t)\approx\left(\frac{1}{t\Gamma(1-\alpha)}\right).$$

Integrals in the complex plane can be simplified using variants of the residue theorem. Assuming $f(s)$ is analytical for $s>0$, and $s\to\infty\Rightarrow f(s)\to 0$ it states that

$$\int_{-i\infty}^{i\infty}\frac{ds_1}{2\pi i}\frac{f(s_1)}{(s-s_1)}=f(s). \tag{A2}$$

APPENDIX B: WAITING-TIME DISTRIBUTION WITH FINITE MEAN AND DIVERGING SECOND MOMENT

An interesting type of subexponential relaxation is the WTD with finite mean $\bar{t}<\infty$ but infinite higher moments, e.g., $\langle t^2\rangle=\infty$ [68]. The typical WTD has the asymptotic form $\psi(t)\approx t^{-1-\alpha}$ with $2>\alpha>1$. The asymptotic form at $s=0$ is connected to moments as $\psi(s)\approx 1-s\bar{t}+s^2\langle t^2\rangle+\cdots$ we therefore look for WTDs with $\psi(s)\approx 1-s+s^\alpha$ at $s=0$.

Consider the following example:

$$\psi_{WAD}(s)=\frac{1}{1+\kappa_1 s/[1+(\kappa_\alpha s)^{\alpha-1}]},$$

$$\psi'_{WAD}(s) = \frac{1}{1 + \kappa_1 s + (\kappa_\alpha s)^{\alpha-1}},$$

which gives for $s \to 0$

$$\psi_{WAD}(s) = 1 - \kappa_1 s + \kappa_1 \kappa_\alpha^{\alpha-1} s^\alpha,$$

$$\psi'_{WAD}(s) = 1 - (\kappa_\alpha s)^{\alpha-1},$$

or in the time domain

$$\psi_{WAD}(t) \propto \kappa_\alpha^{\alpha-1}\kappa_1/t^{\alpha+1}, \quad \psi'_{WAD}(t) \propto \kappa_\alpha^{\alpha-1}/t^\alpha, \quad t \to \infty,$$

while

$$\psi_{WAD}(s) = \kappa_\alpha^{\alpha-1}/(\kappa_1 s^{2-\alpha}), \quad \psi'_{WAD}(s) = 1/(\kappa_1 s), \quad s \to \infty,$$

$$\psi_{WAD}(t) \propto \kappa_\alpha^{\alpha-1}/(\kappa_1 t^{\alpha-1}), \quad \psi'_{WAD}(t) \propto 1/\kappa_1, \quad t \to 0. \tag{B1}$$

The application to a CTRW in a potential gives

$$C(s) = \frac{1 + (D/\sigma^2)\kappa_\alpha(\kappa_\alpha s)^{\alpha-2}}{s + (D/\sigma^2)[1 + (\kappa_\alpha s)^{\alpha-1}]}.$$

The asymptotic form at $s=0$,

$$C(s) = \kappa_\alpha^\alpha s^{\alpha-2},$$

predicts algebraic tails with $t^{\alpha-2}$ in the asymptotic regime.

The correlation function does not depend on κ_1, similar to the results of the main text. This connects to the standard diffusion limit where the entire WTD is scaled with the length of the step a keeping the ratio $a^2/\bar{t}$ constant, and an exponential relaxation is obtained for any SP CTRW. For anomalous relaxation the short time scale κ_1 (κ for TAD) is limited to 0, keeping D, κ_α (D, λ for TAD) constant.

APPENDIX C: THREE-POINT CORRELATION FUNCTIONS

Equations (44) and (45) can be solved by performing a Laplace transform:

$$\hat{R}^{(k)}(s_k; s_{k-1}x_{k-1}, \ldots, s_1x_1) = \int_{\tau_0}^{\infty} \cdots \int_{\tau_{n-1}}^{\infty} \exp\Big(-\sum_{j=1}^{k} s_j(\tau_j - \tau_{j-1})\Big)\hat{R}^{(k)}(\tau_k, \tau_0; \tau_{k-1}x_{k-1}, \ldots, \tau_1x_1)d\tau_k \cdots d\tau_1.$$

s_k are Laplace conjugates to the interval $t_k = \tau_k - \tau_{k-1}$. Laplace transforms for $\hat{\Xi}^{(k)}, \hat{\Psi}, \hat{\Phi}, \hat{\mathcal{G}}^{(k)}$ are defined similarly. Equations (44) and (45) are then transformed to

$$\hat{R}^{(k)}(s_k; s_{k-1}x_{k-1}, \ldots, s_1x_1) = [1 - \hat{\Psi}(s_k)]^{-1}\hat{\Xi}^{(k)}(s_k; s_{k-1}x_{k-1}, \ldots, s_1x_1), \tag{C1}$$

$$\hat{\Xi}^{(k)}(s_k; s_{k-1}x_{k-1}, \ldots, s_1x_1) = \int_{-i\infty}^{i\infty} \frac{ds_k^*}{2\pi i}\hat{\Psi}'(s_k^*)\prod_{q=1}^{k}\frac{1}{s_q - s_k^*}\prod_{q=1}^{k-1}\hat{\Theta}(x_q) + \sum_{j=1}^{k-1}\int_{-i\infty}^{i\infty}\int_{-i\infty}^{i\infty}\frac{ds_j'}{2\pi i}\frac{ds_k^*}{2\pi i}\hat{\Psi}(s_k^*)\left(\frac{1}{s_j - s_j'} - \frac{1}{s_j - s_k^*}\right)$$
$$\times \frac{1}{(s_j' - s_k^*)}\prod_{q=j+1}^{k}\frac{\hat{\Theta}(x_{q-1})}{s_q - s_k^*}\hat{R}^{(j)}(s_j'; s_{j-1}x_{j-1}, \ldots, s_1x_1). \tag{C2}$$

Equation (C2) is simplified using the residue theorem Eq. (A2):

$$\hat{\Xi}^{(k)}(s_k; s_{k-1}x_{k-1}, \ldots, s_1x_1) = \sum_{l=1}^{k}\frac{\hat{\Psi}'(s_l)}{\prod_{q=1;\neq l}^{k}(s_q - s_l)}\prod_{q=1}^{k-1}\hat{\Theta}(x_q) + \sum_{j=1}^{k-1}\sum_{l=j}^{k}\frac{\hat{\Psi}(s_l)}{\prod_{q=j,\neq l}^{k}(s_q - s_l)}\prod_{q=j+1}^{k}\hat{\Theta}(x_{q-1})\hat{R}^{(j)}(s_j; s_{j-1}x_{j-1}, \ldots, s_1x_1). \tag{C3}$$

In a similar way we get the Laplace space form of Eq. (46):

$$\hat{\mathcal{G}}^{(n+1)}(s_n; s_{n-1}x_{n-1}, \ldots, s_1x_1) = \int_{-i\infty}^{i\infty}\frac{ds_n^*}{2\pi i}\hat{\Phi}'(s_n^*)\prod_{q=1}^{n}\frac{1}{s_q - s_n^*}\prod_{q=1}^{n-1}\hat{\Theta}(x_q) + \hat{\Phi}(s_n)\hat{\Theta}(x_n)\hat{R}^{(n)}(s_n; s_{n-1}x_{n-1}, \ldots, s_1x_1)$$
$$+ \sum_{k=1}^{n-1}\int_{-i\infty}^{i\infty}\frac{ds_k'}{2\pi i}\int_{-i\infty}^{i\infty}\frac{ds_n^*}{2\pi i}\hat{\Phi}(s_n^*)\left(\frac{1}{s_k - s_k'} - \frac{1}{s_k - s_n^*}\right) \times \frac{1}{(s_k' - s_n^*)}\prod_{q=k+1}^{n}\frac{1}{s_q - s_n^*}\hat{\Theta}(x_{q-1})$$
$$\times \hat{R}^{(k)}(s_k'; s_{k-1}x_{k-1}, \ldots, s_1x_1). \tag{C4}$$

This gives

$$\hat{\mathcal{G}}^{(n+1)}(s_n;s_{n-1}x_{n-1},\ldots,s_1x_1)=\sum_{l=1}^{n}\frac{\hat{\Phi}'(s_l)}{\prod_{q=1;\neq l}^{n}(s_q-s_l)}\prod_{q=1}^{n-1}\hat{\Theta}(x_q)+\hat{\Phi}(s_n)\hat{R}^{(n)}(s_n;s_{n-1}x_{n-1},\ldots,s_1x_1)$$
$$+\sum_{j=1}^{n-1}\sum_{l=j}^{n}\frac{\hat{\Phi}(s_l)}{\prod_{q=j,\neq l}^{n}(s_q-s_l)}\prod_{q=j+1}^{n}\hat{\Theta}(x_{q-1})\hat{R}^{(j)}(s_j;s_{j-1}x_{j-1},\ldots,s_1x_1). \tag{C5}$$

Direct application of Eq. (C3) gives

$$\hat{\Xi}^{(1)}(s_1)=\hat{\Psi}'(s_1) \tag{C6}$$

and

$$\hat{R}^{(1)}(s_1)=[1-\hat{\Psi}(s_1)]^{-1}\hat{\Psi}'(s_1)$$

and using Eq. (C5) the Green's function Eq. (9) is obtained. The PDFs are finally given by

$$P^{(2)}(s_1x_1,x_0)=\phi'(s_1)\delta_{x_1,x_0}+\langle x_1|\hat{\Phi}(s_1)[1-\hat{\Psi}(s_1)]^{-1}\hat{\Psi}'(s_1)|x_0\rangle\rho_{x_0}(\tau_0). \tag{C7}$$

Other two-point quantities are calculated from Eq. (C7).

We next calculate the three-point quantities

$$\hat{\Xi}^{(2)}(s_2;s_1x_1)=\frac{\hat{\Psi}'(s_1)-\hat{\Psi}'(s_2)}{(s_2-s_1)}\hat{\Theta}(x_1)+\frac{\hat{\Psi}(s_1)-\hat{\Psi}(s_2)}{(s_2-s_1)}\hat{\Theta}(x_1)[1-\hat{\Psi}(s_1)]^{-1}\hat{\Psi}'(s_1). \tag{C8}$$

With Eq. (C8) we prove that the conditions Eqs. (11) and (12) define the stationary model. By applying $\hat{\Xi}^{(2)}$ to the initial density and summing over results of the first measurements $\Sigma_{x_1}\hat{\Xi}^{(2)}(s_2,s_1x_1)\rho(\tau_0)$ we obtain the WTD of the first jump after the second measurement, i.e., the WTD for the first jump after τ_1. We require Eqs. (11) and (12) to hold and after some of algebra we get

$$\sum_{x_1}\hat{\Xi}^{(2)}(s_2,s_1x_1)\rho(\tau_0)=\frac{\hat{\Psi}'(s_2)}{s_1}\rho(\tau_0). \tag{C9}$$

The equilibrium density and the first-jump WTD ψ' are recovered at τ_1 [compare Eq. (C6)]. Therefore, the model is stationary—there is no difference in starting the process at any time.

Combining Eq. (C1) with Eq. (C8) we get

$$\hat{R}^{(2)}(s_2;s_1x_1)=[1-\hat{\Psi}(s_2)]^{-1}\frac{\hat{\Psi}'(s_1)-\hat{\Psi}'(s_2)}{(s_2-s_1)}\hat{\Theta}(x_1)+[1-\hat{\Psi}(s_2)]^{-1}\frac{\hat{\Psi}(s_1)-\hat{\Psi}(s_2)}{(s_2-s_1)}\hat{\Theta}(x_1)[1-\hat{\Psi}(s_1)]^{-1}\hat{\Psi}'(s_1). \tag{C10}$$

Three-point quantities are obtained by applying Eqs. (C1), (C3), and (C5). The PDF is finally given by

$$P^{(3)}(s_2x_2,s_1x_1,x_0)=\Bigg(\frac{\phi'(s_2)-\phi(s_1)'}{s_1-s_2}\delta_{x_2x_1}\delta_{x_1x_0}+\langle x_2|\hat{\Phi}(s_2)[1-\hat{\Psi}^{(2)}(s_2)]^{-1}\frac{[\hat{\Psi}'(s_1)-\hat{\Psi}'(s_2)]}{s_2-s_1}|x_1\rangle\delta_{x_1x_0}+\delta_{x_2x_1}\frac{\phi(s_2)-\phi(s_1)}{s_1-s_2}$$
$$\times\langle x_1|[1-\hat{\Psi}(s_1)]^{-1}\hat{\Psi}'(s_1)|x_0\rangle+\langle x_2|\hat{\Phi}(s_2)[1-\hat{\Psi}(s_2)]^{-1}\frac{[\hat{\Psi}(s_2)-\hat{\Psi}(s_1)]}{s_1-s_2}|x_1\rangle\langle x_1|[1-\hat{\Psi}(s_1)]^{-1}\hat{\Psi}'(s_1)$$
$$\times|x_0\rangle\Bigg)\rho_{x_0}(\tau_0). \tag{C11}$$

Applying Eq. (2) we obtain Eq. (48) and for the SP [Eq. (12)] we get Eq. (49) of the main text.

APPENDIX D: CORRELATION FUNCTION FOR A CTRW IN AN EXTERNAL POTENTIAL

In this appendix we calculate the correlation function for a CTRW, with the diffusion model Eq. (23) and an arbitrary WTD. First we consider a general potential. Starting from the general Green's function for SP diffusion in a potential [Eq. (29)] the correlation function can be calculated by

$$C(s)=\frac{1}{s}\sum_{n=0}^{\infty}\left(1-\frac{\varepsilon_n}{sD^{-1}+s\varepsilon_n\bar{t}\psi(s)/[1-\psi(s)]}\right)\iint dx\,dx'\,x'x\varphi_n(x')\varphi_n'(x)\rho_x(\tau_0) \tag{D1}$$

and δf is the correlation function;

$$B_{SP}^{(2)}(s) = \sum_{n=1}^{\infty} \frac{1}{s}\left[1 - \frac{\varepsilon_n}{sD^{-1} + s\varepsilon_n \bar{t}\psi(s)/[1-\psi(s)]}\right] \iint dx\, dx'\, e^{\beta(x'+x)} \varphi_n(x') \varphi_n'(x) \rho_x(\tau_0) \tag{D2}$$

for an arbitrary potential.

For a harmonic potential Eq. (30) the equilibrium state has a Gaussian form,

$$\rho_x(\tau_0) = \frac{\exp[-x^2/2\sigma^2]}{\sqrt{2\pi}\sigma},$$

where $\sigma^2 = kT/M\Omega^2$, and the Fokker-Planck operator takes the form

$$\hat{\mathcal{L}} = \left(\frac{\partial^2}{\partial x^2} + \frac{1}{\sigma^2}\frac{\partial}{\partial x}x\right),$$

with eigenvalues

$$\varepsilon_n = \frac{n}{\sigma^2}, \tag{D3}$$

right eigenvectors

$$\varphi_n(x) = \frac{\exp(-x^2/2\sigma^2)}{2^n\sqrt{2\pi}n!\,\sigma} H_n\left(\frac{x}{\sigma\sqrt{2}}\right), \tag{D4}$$

where H_n is the nth-order Hermite polynomial

$$H_n(x) \equiv (-1)^n e^{x^2} \frac{d^n}{dx^n} e^{-x^2}, \tag{D5}$$

and left eigenvectors

$$\varphi_n'(x) = H_n\left(\frac{x}{\sigma\sqrt{2}}\right). \tag{D6}$$

Equations (D3)–(D6) are essential to represent the Green's function for a harmonic potential in space variables:

$$\hat{\mathcal{G}}_{x'x}(s) = \frac{1}{s}\sum_n \left(1 - \frac{n}{s\sigma^2 D^{-1} + sn\bar{t}\psi(s)/[1-\psi(s)]}\right) \times \frac{\exp(-x'^2/2\sigma^2)}{2^n\sqrt{2\pi}n!\,\sigma} H_n\left(\frac{x'}{\sigma\sqrt{2}}\right) H_n\left(\frac{x}{\sigma\sqrt{2}}\right). \tag{D7}$$

Combining Eq. (D7) with the TAD model [Eq. (17)] we get Eq. (31).

Calculation of the correlation function is simplified in the harmonic case because the important recurrence relation

$$xH_n(x) = \frac{H_{n+1}(x)}{2} + nH_{n-1}(x) \tag{D8}$$

enables a simple representation of $\hat{x}$:

$$\hat{x}|\varphi_n\rangle = \sigma\sqrt{2}\left((n+1)|\varphi_{n+1}\rangle + \frac{1}{2}|\varphi_{n-1}\rangle\right).$$

For a harmonic potential, space integration for the correlation function is simplified:

$$C(s) = \frac{\sigma^2}{s}\frac{[1-\psi(s)] + D\bar{t}[\psi(s) - \psi'(s)]/\sigma^2}{[1-\psi(s)] + D\bar{t}\psi(s)/\sigma^2} \tag{D9}$$

and by applying the stationary condition [Eq. (12)],

$$C(s) = \frac{\sigma^2}{s}\left(1 - \frac{1}{s\{\sigma^2 D^{-1} + \bar{t}\psi(s)/[1-\psi(s)]\}}\right). \tag{D10}$$

Combining with Eq. (17) we recover Eq. (33).

In principle, $\psi(s)$ can be reconstructed once $C(s)$ is known. The other parameters are found as $\sigma^2 = C(t=0)$ and using

$$\lim_{s\to\infty} \frac{\bar{t}\psi(s)}{1-\psi(s)} = 0,$$

we get $D = \lim_{s\to\infty}[s\sigma^2 - s^2 C(s)]$. Equation (D10) then gives ψ. Using $C(t)$ the CTRW model is reconstructed and may be further tested.

The general scheme for probing the multipoint quantities is as follows: $B^{(2)}(t) \rightarrow$ parameters of models [ψ (SP) or $C(t)$ (GP)] $\rightarrow$ prediction $B^{(k\geq 3)}(t)$ and experimental test. In practice, a small number of parameters will be fitted to parametrize the WTD (in our model α, κ, λ). The quality of such fits is not enough to distinguish between a CTRW and the Gaussian model, but higher-order correlation functions are important.

Higher moments of x are calculated by using a convenient representation of $\hat{x}$ in terms of creation and annihilation operators:

$$\hat{x} = \sigma(b^\dagger + b),$$

$$b^\dagger|\varphi_n\rangle = \sqrt{2}(n+1)|\varphi_{n+1}\rangle,$$

$$b|\varphi_n\rangle = \frac{1}{\sqrt{2}}|\varphi_{n-1}\rangle.$$

For an arbitrary function $Q(x)$,

$$\int_{\tau_0}^{\infty} d\tau_1 e^{-s(\tau_1-\tau_0)}\langle Q(x(\tau_1))Q(x(\tau_0))\rangle = \langle\varphi_0'|Q(b+b^\dagger)\hat{G}(s)Q(b+b^\dagger)|\varphi_0\rangle.$$

Using the relation

$$\exp -\beta\hat{x} = e^{(\beta\sigma)^2/2}\exp -\beta b^\dagger \exp -\beta b$$

we get

$$B^{(2)}(s) = e^{(\beta\sigma)^2}\sum_{n=1}^{\infty}\frac{(\beta\sigma)^{2n}}{n!}\frac{1}{s} \times\frac{[1-\psi(s)]+D\bar{t}n[\psi(s)-\psi'(s)]/\sigma^2}{[1-\psi(s)]+D\bar{t}n\psi(s)/\sigma^2} \quad \text{(D11)}$$

and applying the stationary condition [Eq. (12)],

$$B^{(2)}(s) = \exp(\beta\sigma)^2\sum_{n=1}^{\infty}\frac{(\beta\sigma)^{2n}}{n!}\frac{1}{s} \times\left(1-\frac{1}{s\{\sigma^2/nD+\bar{t}\psi(s)/[1-\psi(s)]\}}\right), \quad \text{(D12)}$$

which gives Eq. (38) by applying Eq. (17).

The three-point PDF for the diffusion potential is

$$\begin{aligned}P(s_2x_2,s_1x_1,x_0) &= \frac{\phi'(s_2)-\phi'(s_1)}{s_1-s_2}\delta(x_2-x_1)\delta(x_1-x_0)\rho_{x_0}(\tau_0)+\sum_{k=0}^{\infty}\frac{\phi(s_2)[\psi'(s_1)-\psi'(s_2)](1-\varepsilon_k D\bar{t})}{[1-\psi(s_2)(1-\varepsilon_k D\bar{t})](s_2-s_1)}\varphi_k(x_2)\varphi_k'(x_1)\delta(x_1-x_0)\rho_{x_0}(\tau_0)\\ &+\sum_{n=0}^{\infty}\frac{[\phi(s_2)-\phi(s_1)](1-\varepsilon_n D\bar{t})\psi'(s_1)}{(s_1-s_2)[1-\psi(s_1)(1-\varepsilon_n D\bar{t})]}\delta(x_2-x_1)\varphi_n(x_1)\varphi_n'(x_0)\rho_{x_0}(\tau_0)\\ &+\sum_{k=0}^{\infty}\sum_{n=0}^{\infty}\frac{\phi(s_2)[\psi(s_2)-\psi(s_1)](1-\varepsilon_k D\bar{t})(1-\varepsilon_n D\bar{t})\psi'(s_1)}{[1-(1-\varepsilon_k D\bar{t})\psi(s_2)](s_1-s_2)[1-(1-\varepsilon_n D\bar{t})\psi(s_1)]}\varphi_k(x_2)\varphi_k'(x_1)\varphi_n(x_1)\varphi_n'(x_0)\rho_{x_0}(\tau_0). \quad \text{(D13)}\end{aligned}$$

The three-point correlation function $\mathcal{B}^{(3)}\equiv\langle\exp[\beta x(\tau_2)]\exp[\beta x(\tau_1)]\exp[\beta x(\tau_0)]\rangle$ for the SP may by calculated by

$$\begin{aligned}\mathcal{B}^{(3)}(s_2,s_1) &= \exp[3(\beta\sigma)^2/2]\sum_{k=0}^{\infty}\sum_{m=0}^{\infty}\sum_{j=0}^{\infty}\frac{(\beta\sigma)^{2(m+k+j)}}{m\,!\,k\,!\,j!}\times\left(\frac{1}{s_1s_2}-\frac{1}{s_1s_2^2\left(\frac{\bar{t}\psi(s_2)}{[1-\psi(s_2)]}+\frac{\sigma^2}{(j+k)D}\right)}-\frac{1}{s_2s_1^2\left(\frac{\bar{t}\psi(s_1)}{[1-\psi(s_1)]}+\frac{\sigma^2}{(j+m)D}\right)}\right.\\ &\left.+\frac{\psi(s_2)-\psi(s_1)}{(s_1-s_2)s_1s_2\bar{t}\left(\psi(s_2)+\frac{\sigma^2[1-\psi(s_2)]}{(j+k)D\bar{t}}\right)\left(\psi(s_1)+\frac{\sigma^2[1-\psi(s_1)]}{(j+m)D\bar{t}}\right)}\right). \quad \text{(D14)}\end{aligned}$$

Equation (52) is obtained by applying Eq. (17) to Eq. (D14).

APPENDIX E: NONSTATIONARY CTRW

The results of Appendix C are applicable to nonstationary processes, except that the WTD for the first jump is different from Eq. (12). In the general case, the first measurement is not made at the start of the nonstationary process and the two-time PDF $P^{(2)}(\tau_1x_1,\tau_0x_0)$ depends on the time t_0 between the start of the process and the first measurement. One way is to calculate C from the three-time PDF:

$$C(\tau_2x_2,\tau_1x_1)=\int P(x_2\tau_2,x_1\tau_1,x_0\tau_0)dx_0.$$

A simpler approach is to calculate the changed WTD for the very first jump from the time of the first measurement $\psi^{(1)}$ dependent on t_0,

$$\psi^{(1)}(s_1,s_0)=\frac{\psi(s_1)-\psi(s_0)}{s_0-s_1}\frac{\psi'(s_0)}{1-\psi(s_0)}+\frac{\psi'(s_1)-\psi'(s_0)}{s_0-s_1}. \quad \text{(E1)}$$

For the stationary process we set $\psi'(s)=[1-\psi(s)]/s\bar{t}$; and get the waiting-time function independent on the time interval t_0, as expected for a stationary process:

$$\psi^{(1)}(s_1,s_0)=\frac{1-\psi(s_1)}{s_0s_1\bar{t}}, \quad \psi^{(1)}(s_1,\tau_0)=\frac{1-\psi(s_1)}{s_1\bar{t}}=\psi'(s_1).$$

In contrast the correlation function for a nonstationary process with $\psi'(s)=\psi(s)$ carries information about the starting time, and will depend on both time intervals,

$$\psi^{(1)}(s_1,s_0)=\frac{\psi(s_1)-\psi(s_0)}{s_0-s_1}\frac{1}{1-\psi(s_0)}.$$

If the first measurement is made at the time origin, the WTD is not special but $\psi(s)=\psi'(s)$. This refers to the commonly used NP, which is compared to the SP in the main text. Below we focus on the NP. The Green's function Eq. (10) is

$$\hat{\mathcal{G}}(s)=\frac{1}{s\{\hat{1}-D\bar{t}\psi(s)\hat{\mathcal{L}}/[1-\psi(s)]\}} \quad \text{(E2)}$$

which is the Green's function of the Fokker-Planck equation for $\psi(s)=\lambda/(s+\lambda)$ and the Green's function of the FFPE for $\psi(s)=1/(1+s^{\alpha})$.

Expanded in the eigenbasis of the Fokker-Planck operator the Green's function takes the form

$$\hat{\mathcal{G}}_{x'x}(s) = \frac{1}{s}\sum_{n=0}^{\infty} \frac{1-\psi(s)}{[1-\psi(s)] + D\bar{t}\varepsilon_n \psi(s)/\sigma^2} \varphi_n(x)\varphi_n'(x'). \tag{E3}$$

The correlation function is given by

$$C(s) = (\sigma^2/s)\frac{1-\psi(s)}{[1-\psi(s)] + D\bar{t}\psi(s)/\sigma^2}. \tag{E4}$$

The δf correlation function is calculated using

$$B_{NP}^{(2)}(s) = \exp(\beta\sigma)^2 \sum_{n=1}^{\infty} \frac{(\beta\sigma)^{2n}}{n!} \frac{1}{s + nsD\bar{t}\psi(s)/\sigma^2[1-\psi(s)]}. \tag{E5}$$

As the NP is treated in the context of the WTD with $\bar{t} = \infty$ one should replace $D\bar{t} \to a^2/2$. For the Mittag-Leffler model Eq. (14)

$$\frac{D\bar{t}\psi(s)}{[1-\psi(s)]} = \frac{a^2 s^{-\alpha}}{\kappa^\alpha}$$

and with the definition

$$D_\alpha \equiv \frac{a^2}{2\kappa^\alpha}$$

Eq. (E2) becomes the Green's function for the fractional Fokker-Planck equation [7]. Equations (E3), (E4), and (E5) correspond to Eqs.(32), (34), and (39), respectively.

[1] H. Risken, *The Fokker-Plank Equation* (Springer, Berlin, 1989).
[2] G. H. Weiss, *Aspects and Applications of the Random Walks* (North-Holland, Amsterdam, 1994).
[3] N. Wiener, J. Math. Phys. (Cambridge, Mass.) **2**, 131 (1923).
[4] B. B. Mandelbrot, *The Fractal Geometry of Nature* (Freeman, San Francisco, 1983).
[5] M. F. Shlesinger, Annu. Rev. Phys. Chem. **39**, 269 (1988).
[6] J.-P. Bouchard and A. Georges, Phys. Rep. **195**, 127 (1990).
[7] R. Metzler and J. Klafter, Phys. Rep. **339**, 1 (2000).
[8] R. Metzler and J. Klafter, J. Phys. A **37**, R161 (2004).
[9] A. M van Oijen, P. C. Blatney, D. J. Crampton, Ch .C. Richardson, T. Ellenberger, and X. S. Xie Science **301**, 1235 (2003).
[10] H. Yang, G. Luo, P. Karnchanaphanurach, T-M. Louie, I. Rech, S. Cova, L. Xun, and X. S. Xie, Science **302**, 262 (2003).
[11] O. Flomenbom, K. Velonia, D. Loos, S. Masuo, M. Cotlet, Y. Engelborghs, Hofkens, A. E. Rowan, R. J. M. Nolte, F. C. de Schryver, and J. Klafter, Proc. Natl. Acad. Sci. U.S.A. **102**, 2368 (2005).
[12] L. Edman, Z. Földes-Papp, S. Wennmalm, and R. Rigler, Chem. Phys. **247**, 11 (1999).
[13] G. Zumofen,J. Klafter, Chem. Phys. Lett. **219**, 303 (1994).
[14] M. Kuno, D. P. Fromm, H. F. Hamman, A. Gallagher, and D. J. Nesbitt, J. Chem. Phys. **112**, 3117 (2000).
[15] K. T. Shimizu, R. G. Neuhauser, C. A. Leatherdale, S. A. Empedocles, W. K. Woo, and M. G. Bawendi, Phys. Rev. B **63**, 205316 (2001).
[16] B. R. Fisher, H. J. Eisler, N. E. Stott, and M. G. Bawendi, J. Phys. Chem. B **108**, 143 (2004).
[17] G. Schlegel, J. Bohnenberger, I. Potapova, and A. Mews, Phys. Rev. Lett. **88**, 137401 (2002).
[18] M. Kuno, D. P. Fromm, S. T. Johnson, A. Gallagher, and D. J. Nesbitt, Phys. Rev. B **67**, 125304 (2003).
[19] M. Kuno, D. P. Fromm, H. F. Hamman, A. Gallagher, and D. J. Nesbitt, J. Chem. Phys. **115**, 1028 (2001).
[20] G. Messin, J. P. Hermier, E. Giacobino, P. Desbioles, and M. Dahan, Opt. Lett. **26**, 1891 (2001).
[21] S. S. Plotkin and P. G. Wolynes, Proc. Natl. Acad. Sci. U.S.A. **100**, 4417 (2003).
[22] J. N. Onuchic, Z. Luthey-Schulten, and P. G. Wolynes, Annu. Rev. Phys. Chem. **48**, 545 (1997).
[23] I. M. Sokolov, J. Klafter, and A. Blumen, Phys. Today **55** (11), 48 (2002).
[24] G. Margolin and E. Barkai, J. Chem. Phys. **121**, 1566 (2004).
[25] G. Margolin and E. Barkai, Phys. Rev. Lett. **94**, 080601 (2005).
[26] V. Barsegov and S. Mukamel, J. Phys. Chem. B **108**, 15 (2004).
[27] S. C. Kou and X. S. Xie, Phys. Rev. Lett. **93**, 180603 (2004).
[28] W. Min, G. Luo, B. J. Cherayil, S. C. Kou, and S. X. Xie, Phys. Rev. Lett. **94**, 198302 (2005).
[29] H. Quian, in *Processes with Long-Range Correlations: Theory and Applications*, edited by G. Rangarajan and M. Z. Ding, Lecture Notes in Physics Vol. 621 (Springer, New York, 2003), p. 22.
[30] B. O'Shaughnessy and I. Procaccia, Phys. Rev. Lett. **54**, 455 (1985).
[31] F. E. Peseckis, Phys. Rev. A **36**, 892 (1987).
[32] K. G. Wang and M. Tokuyama, Physica A **65**, 341 (1999).
[33] V. M. Kenkre, E. W. Montroll, and M. F. Shlesinger, J. Stat. Phys. **9**, 45 (1973).
[34] D. T. Gillespie, Phys. Lett. **64A**, 22 (1977).
[35] M. O. Vlad, V. T. Popa, and E. Segal, Phys. Lett. **100A**, 387 (1984).
[36] M. O. Vlad and A. Pop, Physica A **155**, 276 (1989).
[37] J. W. Haus and K. W. Kehr, Phys. Rep. **150**, 263 (1987).
[38] R. F. Fox, Phys. Rep. **48**, 179 (1978).
[39] F. Bardou, J. P. Bouchard, A. Aspect, and C. Cohen-Tanoudji, *Lévy Statistics and Laser Cooling: How Rare Events Bring Atoms to Rest* (Cambridge University Press, Cambridge, U.K., 2002).
[40] W. E. Montroll and G. H. Weiss, J. Math. Phys. **6**, 167 (1965).
[41] H. Scher and M. Lax, Phys. Rev. B **7**, 4491 (1973); **7**, 4502 (1973).
[42] D. Bedeaux, K. Lakatos-Lindenberg, and K. Shuler, J. Math. Phys. **12**, 2116 (1971).
[43] F. W. Schmidlin, Phys. Rev. B **16**, 2362 (1977).
[44] J. Noolandi, Phys. Rev. B **16**, 4474 (1977).
[45] K. W. Kehr and J. W. Haus, Physica A **93**, 412 (1978).

[46] D. Gamliel and H. Levanon, *Stochastic Processes in Magnetic Resonance* (World Scientific, River Edge, NJ, 1995).
[47] D. J. Schneider and J. H. Freed, Special issue of Adv. Chem. Phys. **73**, 387 (1989).
[48] D. E. Budil, S. Lee, S. Saxena, and J. H. Freed, J. Magn. Reson., Ser. A **120**, 155 (1996).
[49] A. I. Shushin, Phys. Rev. E **64**, 051108 (2001).
[50] A. I. Shushin, Phys. Rev. E **67**, 061107 (2003).
[51] A. I. Shushin, Physica A **340**, 283 (2004).
[52] H. Scher and W. E. Montroll, Phys. Rev. B **12**, 2455 (1975).
[53] G. F. L. Ferreira, Phys. Rev. B **16**, 4719 (1977)
[54] W. Feller, *An Introduction to Probability Theory and Its Application* (Willey, New York, 1971).
[55] M. Lax and H. Scher, Phys. Rev. Lett. **13**, 781 (1977).
[56] J. K. E. Tunaley, Phys. Rev. Lett. **33**, 1037 (1974).
[57] R. Verberk and M. Orrit, J. Chem. Phys. **119**, 2214 (2003).
[58] Y. Jung, E. Barkai, and R. Silbey, Chem. Phys. **284**, 181 (2002).
[59] E. Barkai, R. Metzler, and J. Klafter, Phys. Rev. E **61**, 132 (2000).
[60] R. Metzler, E. Barkai, and J. Klafter, Phys. Rev. Lett. **82**, 3563 (1999).
[61] H. Yang and S. X. Xie, J. Chem. Phys. **117**, 10965 (2002); Chem. Phys. **284**, 423 (2003).
[62] S. Mukamel, *Principles of Nonlinear Optical Spectroscopy* (Oxford University Press, New York, 1995).
[63] Y. Tanimura and S. Mukamel, J. Chem. Phys. **99**, 9496 (1993).
[64] D. Abramavicius and S. Mukamel, Chem. Rev. (Washington, D.C.) **104**, 2073 (2004).
[65] A. Erdélyi *et al.*, *Higher Transcendental Functions* (McGraw-Hill, New York, 1955), Vol. 3.
[66] G. Mittag-Leffler, Acta Math. **29**, 1019 (1905).
[67] V. Khidekel, V. Chernyak, and S. Mukamel, J. Chem. Phys. **105**, 8543 (1996).
[68] M. F. Shlesinger, J. Stat. Phys. **10**, 421 (1974).